A STATISTICAL STUDY FOR AUTOMATIC CALIBRATION OF A CONCEPTUAL RUNOFF MODEL

STATISTISK STUDIE FÖR AUTOMATISK KALIBRERING AV EN BEGREPPSMÄSSIG AVRINNINGSMODELL

Sören Svensson

SMHI Rapporter

HYDROLOGI OCH OCEANOGRAFI
Nr RHO 10 (1977)

SVERIGES METEOROLOGISKA OCH HYDROLOGISKA INSTITUT

A STATISTICAL STUDY FOR AUTOMATIC CALIBRATION OF A CONCEPTUAL RUNOFF MODEL

STATISTISK STUDIE FÖR AUTOMATISK KALIBRERING AV EN BEGREPPSMÄSSIG AVRINNINGSMODELL

Sören Svensson

SMHI Rapporter

HYDROLOGI OCH OCEANOGRAFI
Nr RHO 10 (1977)

SVERIGES METEOROLOGISKA OCH HYDROLOGISKA INSTITUT

Norrköping 1977

LIST OF CONTENTS

SUMMARY

A conceptual runoff model is studied in this work. Especially the residuals of the model (the differences between the computed hydrograph and the recorded one) are examined. The density function and the autocorrelation function of the residuals are estimated and tested.

The model must be calibrated for each new catchment, to which it is applied. Therefore a criterion of the goodness of fit between the computed and the recorded hydrograph is required. Some criteria of fit have been examined concerning their sensitivity to changes in the model parameter setting.

Conclusions of the work are: The residuals of the model are neither stationary nor independent and normally distributed. A classification based on the different physical processes, which govern the discharge, makes the residuals of each class more stationary and in some sense more normally distributed than the residuals of the material without any classification. Furthermore a criterion of goodness of fit, based on the classification above resembles the subjectively judged fit more than the simple sum of squares criterion, which has become practice in applications of runoff models.

1. INTRODUCTION

The purposes of the development of hydrological catchment models are mainly (Clarke, 1973):

1. Forecasting
   a) Operational forecast: Estimating streamflow when rainfalls, losses, streamflows etc. are given up to the present time.
   b) Design forecast: Estimating the flood hydrograph caused by a hypothetical heavy storm (or snowmelt).
2. Extending the discharge redord, where we have got long climatological record but short discharge record.
3. Prediction of the possible effects of proposed physical changes to the catchment.

Before the model can be taken into operation, its free parameters have to be accurately estimated by means of a calibration procedure. This means that the parameters are adjusted until a good fit is obtained between the computed hydrograph and the observed one. The procedure can be either a subjective one, relying upon the hydrologist when deciding which parameters are to be adjusted, or an automatic one, based on an optimization algorithm.

One major problem concerning the automatic procedure has been the finding of a matching index, a criterion of fit. This is very important, because every automatic parameter optimization routine has to rely upon a numerical value of the goodness of fit between two curves.

The statistical properties of the residuals could be a key to a better understanding of this problem. The lack of such studies was pointed out by Clarke (1973).

Clarke (1973) also stated that if estimated confidence regions for the parameters are required, assumptions must be made about the probability distribution of the model residuals. However, one further possibility is to do a number of parameter estimations based on independent data and from the results of these estimations get an apprehension of the size of the confidence regions of the model parameters.

The aim of this work is to study the statistical properties of the residuals in order to find a more appropriate criterion of fit between the computed and the recorded hydrograph. This problem was approached in two steps.

1. The calibration period was divided into "subperiods" in order to obtain stationary subsets of residuals. Some statistical properties of these residuals were examined.
2. The response surfaces of different criteria of fit were studied when altering the parameter values.

The HBV runoff model was used for the study. This model is developed at the SMHI (Swedish Meteorological and Hydrological Institute) by Bergström (1976). It is in operational use in some catchments in Sweden and Norway.

This study was financed by the SMHI and it was carried out in co-operation with the Department of Mathematics at the Linköping University.

Fig. 2.1. Test catchments for the applications of the study of the HBV model.

2. TEST CATCHMENTS

Two catchments were used in the study: the Kultsjön catchment, below referred to as Kultsjön, and the Stadarforsen catchment, below referred to as Stadarforsen (fig. 2.1). Both catchments are below timberline dominated by coniferous forest, and the soil is mostly moraine or of a pervious type.

The catchments are representative for large areas in Scandinavia.

Table 2.1 Test catchments.

Catchment	River	Area (km^2)	Altitude range (m)	Lakes %
Stadarforsen	Västerdalälven	4 136	835	2,4
Kultsjön	Ångermanälven	1 109	1 040	6

The analysed runoff record of Stadarforsen began 1961-10-01 and ended 1976-03-31. In Kultsjön the analysed record began 1961-10-01 and ended 1976-05-18.

3. THE HBV-MODEL AND ITS FREE PARAMETERS

The simulation of discharge by the HBV-model is made in three steps (fig. 3.1).

1. Snow accumulation and ablation.
2. Soil moisture accounting.
3. Generation of runoff and transformation of the hydrograph.

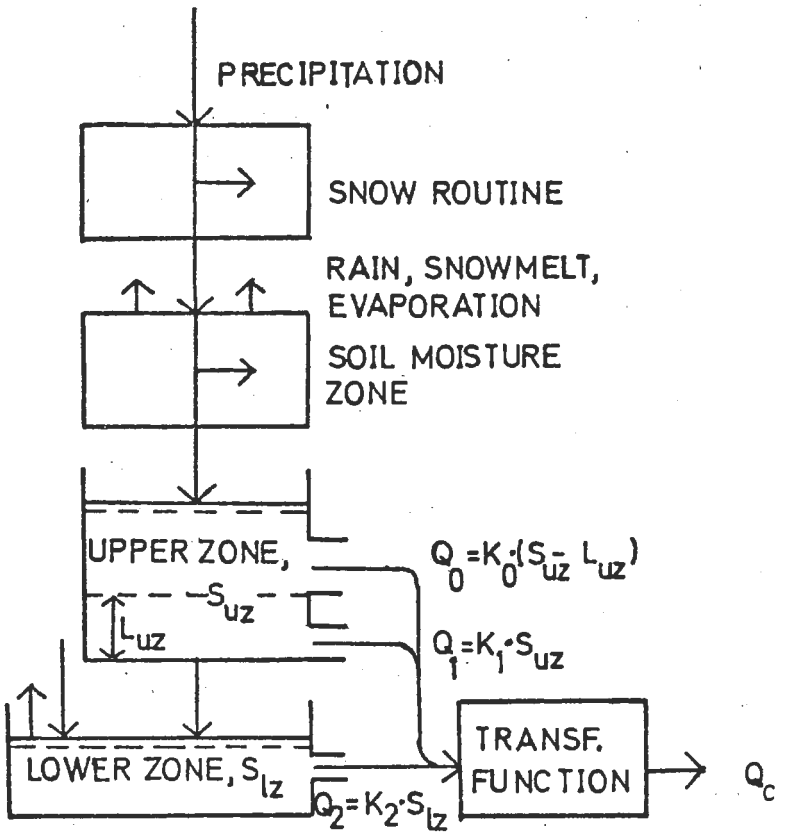

Fig. 3.1 Schematic representation of the HBV-model.

Table 3.1 Parameters of the HBV-model.

Corrections on input variables

P_{corr} = correction factor on rainfall
P_{lapse} = precipitation-elevation correction
T_{lapse} = temperature-elevation correction
T_o = general temperature correction

Parameters of the snowroutine

C_{sf} = snow fall correction factor
C_o = degree-day melt factor
C_{wh} = water holding capacity
S_b = bottom storage under snowpack
C_{rfr} = refreezing coefficient

Parameters of the soil moisture routine

Fc = maximum soil moisture storage
L_p = limit for potential evaporation
β = empirical coefficient

Parameters of the response function

K_o = storage discharge constant of the upper zone
K_1 = " " " " " " "
K_2 = " " " " " lower "
L_{uz} = limit for slow drainage of the upper zone
C_{perc} = percolation capacity into the lower zone
P_w = part of the lower zone representing lakes and other wet areas
B_{max} = maximum base in the transformation function
C_{route} = parameter relating the base in the transformation function to the generated flow

The model parameters are shown in table 3.1. P_{corr}, P_{lapse}, T_{lapse} and P_w are set from information outside the calibration procedure (maps, experience etc.). The others are calibrated to optimum fit.

3.1 Snow routine

Whenever the air temperature (T) is below a threshold value (T_o), all precipitation is regarded as snow and is accumulated in the snowpack.

All effects of evaporation and lacking representativeness of the gauge are put together in one empirical coefficient, the snow fall correction factor (C_{sf}).

Thus, if $T < T_o$ then

$$S_s = C_{sf} \cdot P,$$

where S_s = actual snow accumulation (mm),
C_{sf} = snow fall correction factor,
P = precipitation (mm),
T = surface air temperature (^oC).

Snowmelt is taken care of by the degree-day method:

If $T > T_o$, then

$$M = C_o (T - T_o),$$

where M = snowmelt (mm/day),
C_o = degree-day factor (mm/(^oC day)).

The water retention in the snowpack is described by two parameters.

C_{wh} = waterholding capacity of the snow (% of the snowpack),
S_b = bottom storage under the snow (mm).

S_b has rarely been used and was therefore omitted in this work.

Refreezing of liquid water in the snowpack:

If $T < T_o$ and if there is liquid water present in the snowpack, then

$$M = C_{rfr} \cdot C_o (T - T_o),$$

where $-M$ = refreezing rate (mm/day),
C_{rfr} = refreezing coefficient.

The area-elevation distribution of the snowroutine in the HBV-model is described by Bergström (1976). It contains no free parameters and is therefore not very interesting for the calibration of the model.

3.2 Soil moisture routine

The behaviour of the soil moisture zone is illustrated in fig. 3.2.

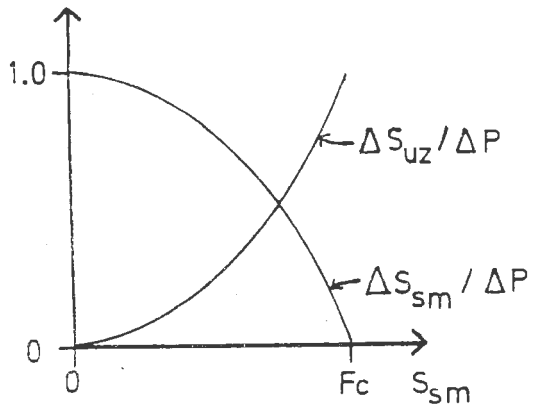

Fig. 3.2 The contributions from rainfall or snowmelt, P, to the soil moisture zone, S_{sm}, and the upper zone, S_{uz}.

Mathematically, this can be described by the following equations:

$$\frac{\Delta S_{uz}}{\Delta P} = \left(\frac{S_{sm}}{Fc}\right)^{\beta}$$

$$\frac{\Delta S_{sm}}{\Delta P} = 1 - \left(\frac{S_{sm}}{Fc}\right)^{\beta}$$

where P = precipitation or snowmelt (mm),

S_{uz} = storage in the upper zone (mm),

S_{sm} = computed soil moisture storage (mm),

Fc = maximum soil moisture storage in the model (mm),

β = empirical coefficient,

ΔS_{uz} = amount that passes through the soil moisture zone (mm),

ΔS_{sm} = amount that is stored in the soil moisture zone (mm),

$\Delta \hat{p}$ = precipitation or snowmelt fed into the zone mm by mm.

Potential evaporation is reduced to actual values by the function in fig. 3.3.

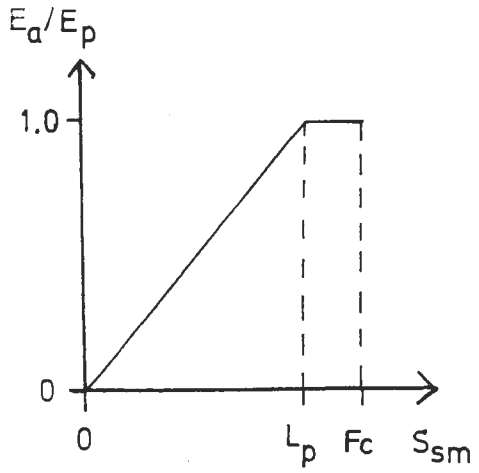

Fig. 3.3 Reduction of potential evaporation, E_p, to actual, E_a.

Mathematically described by:

$$E_a = \begin{cases} E_p \text{ if } S_{sm} \geq L_p \\ E_p \cdot \frac{S_{sm}}{L_p} \text{ if } S_{sm} < L_p, \end{cases}$$

where E_p = potential evaporation,

E_a = actual evaporation,

L_p = limit for potential evaporation.

3.3 Response function

Having passed the soil moisture routine the excess water passes through some reservoirs, where the runoff Q_g is easily calculated in the manner illustrated in fig. 3.4.

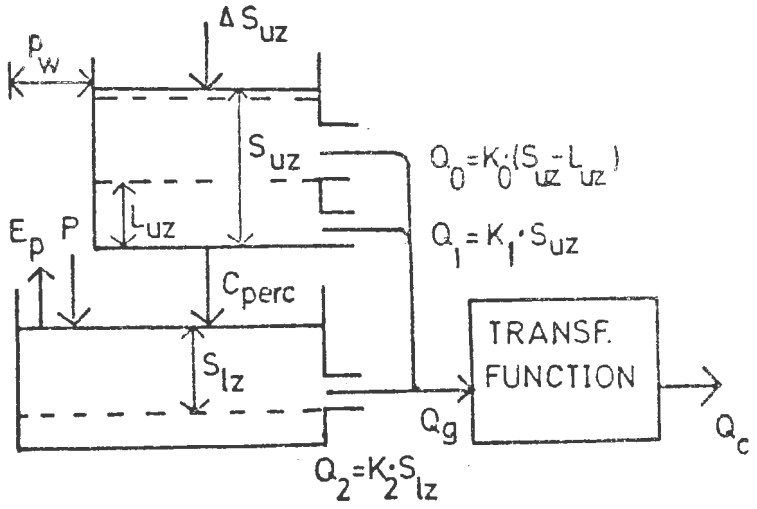

Fig. 3.4 The response function of the HBV-model.

C_{perc} = percolation capacity,
E_p = potential evaporation,
K_o = storage discharge parameter of the upper zone,
K_1 = slow drainage storage discharge parameter of the upper zone,
K_2 = storage discharge parameter of the lower zone,
L_{uz} = limit for slow drainage of the upper zone,
P = precipitation,
P_w = part of the lower zone, representing wet areas,
Q_g = total generated runoff,
Q_o = runoff generated from the upper zone,
Q_1 = slow drainage runoff generated from the upper zone,
Q_2 = runoff generated from the lower zone
Q_c = total computed runoff,
S_{lz} = storage in the lower zone of the model,
S_{uz} = " " " upper " " " "
ΔS_{uz} = inflow in the upper zone.

The transforming function multiplies Q_g with a weight differing in time. Q_g is transformed into Q_c according to fig. 3.5.

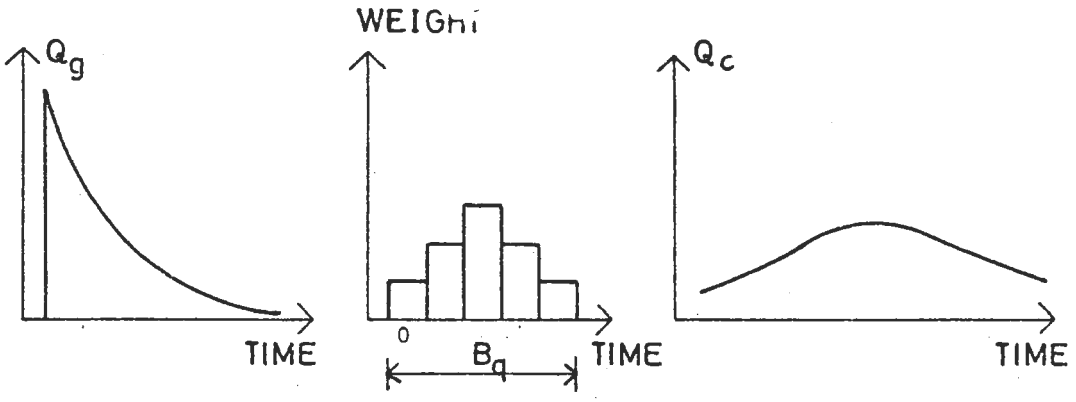

Fig. 3.5 The effect of the transformation function on the generated hydrograph.

This can be expressed as:

$$B_q = \begin{cases} B_{max} - C_{route} \cdot Q_g & \text{if } (B_{max} - C_{route} \cdot Q_g) \geq 1 \\ 1 & \text{if } (B_{max} - C_{route} \cdot Q_g) < 1 \end{cases}$$

B_q = base of the triangular function (days),
B_{max} = maximum base (days),
C_{route} = free parameter (days/(m^3/s)),
Q_g = generated runoff from the reservoirs (m^3/s),
Time = 0: the day on which Q_g is generated (days).

4. STATISTICAL ANALYSIS OF THE RESIDUALS OF THE HBV-MODEL

4.1 Mechanism separation criterion (MSC)

A study of the hydrographs showed that different physical processes produced different discharge patterns. Subsequently a study of the residuals showed a similar mixture of different curve types with different statistical properties.

Chiefly three different processes were assumed.

1. Snowmelt
2. Rainfall or recession succeding rainfall or snowmelt (referred to as γ-flow)
3. Dry summer- or winter-recession (referred to as low flow).

The problem was to find a good criterion to separate the days in order to obtain classes of days with approximately stationary residuals. One method is to divide the calibration period by visual inspection. The drawbacks of this method are its subjective character and the fact that it does not take the different model mechanisms into account.

The method was therefore abandoned and the following mechaism separation criterion (MSC) was used.

1. $M > 0$: snowmelt
2. $M \leq 0$ and ($\Delta S_{uz} > 0$ or $S_{uz} > 0$): γ-flow
3. $M \leq 0$ and ($\Delta S_{uz} = 0$ and $S_{uz} = 0$): low flow,

where M = snowmelt (mm),
S_{uz} = storage in the upper zone of the model (mm),
ΔS_{uz} = inflow in the upper zone of the model (mm).

This MSC has two major drawbacks:

1. It will give different partitions of the calibration period at different parameter settings. This will disturb the behaviour of the properties studied.

2. It may be difficult to apply to other models.

The main advantage of the chosen MSC is that it is easy to extract from the model. An example of the use of the MSC is shown in fig. 4.1.

In Kultsjön the transforming function causes a time lag, which has a maximum length of one day (B_{max} = 2, C_{route} = 0.00103, chapter 3.3). This small influence is neglected in the mechanism separation.

In Stadarforsen the time lag is much greater (B_{max} = 6, C_{route} = 0, chapter 3.3). Here the main part of the generated runoff is delayed by three days. In consequense of this the MSC was displaced three days.

Fig. 4.1 (See next page.) Residuals (l/s) and MSC of Stadarforsen 65.10.01 - 69.09.30.

1. Snowmelt
2. Rain or recession succeeding rain or snowmelt.
3. Dry summer- or winter-recession.

The upper curves show the MSC, the lower curves show the residuals.

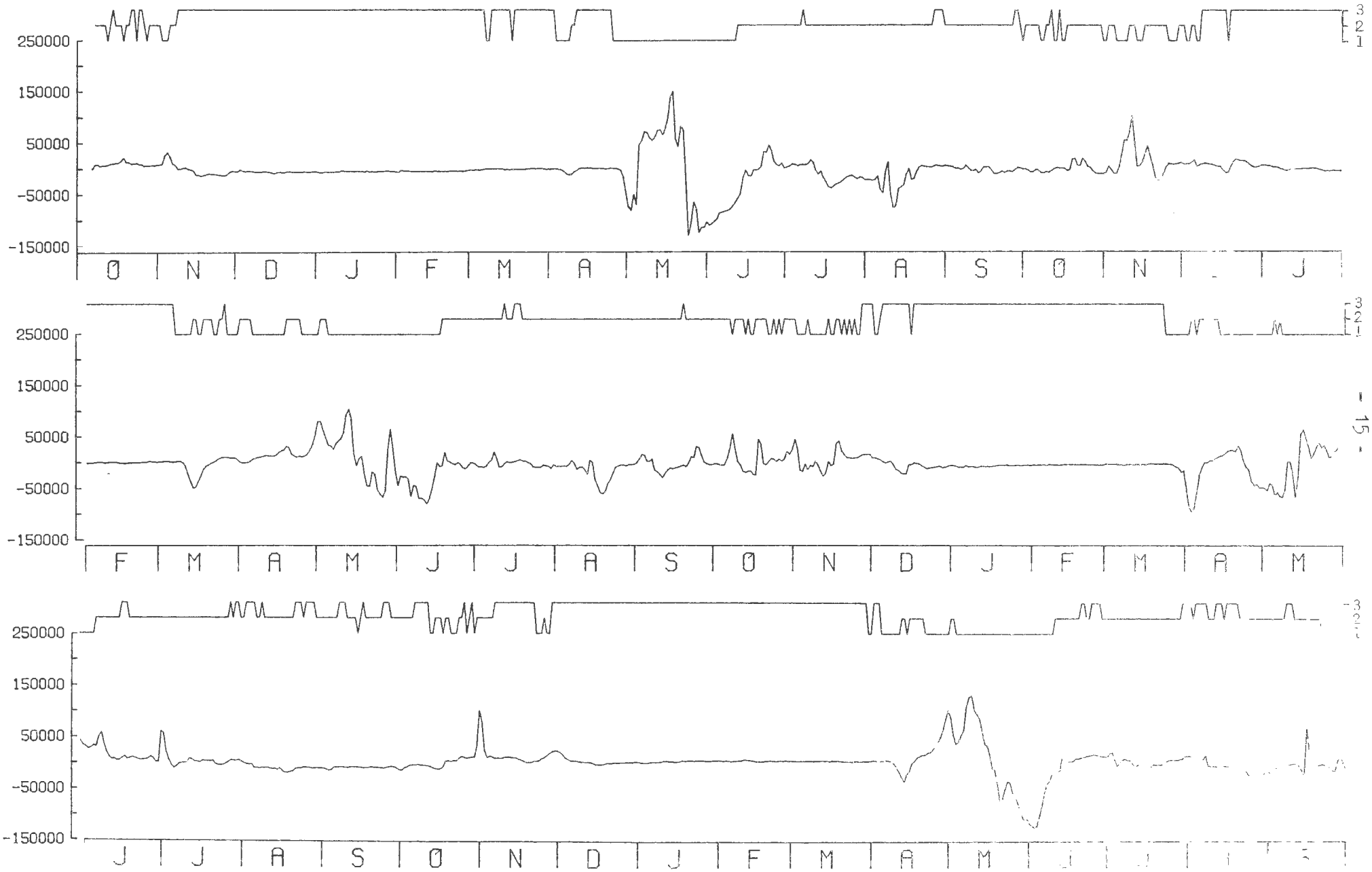
250000
150000
50000
-50000
-150000
O N D J F M A M J J A S O N J
F M A M J J A S O N D J F M A M
J J A S O N D J F M A M

Fig. 4.1

4.2 Estimation of the density function

Mean and standard deviation of the residuals were estimated by:

$$\bar{X} = \frac{1}{n} \sum_{i=o}^{n} \left[Q_r(i) - Q_c(i) \right]$$

$$S^2 = \frac{1}{n-1} \sum_{i=o}^{n} \left[Q_r(i) - Q_c(i) - \bar{X} \right]^2$$

where $\bar{X}$ = mean value of the chosen residuals (m^3/s),
n = number of the chosen residuals,
$Q_r(i)$ = observed discharge (m^3/s),
$Q_c(i)$ = computed discharge (m^3/s),
S = standard deviation of the chosen residuals (m^3/s).

A symmetrical interval, four standard deviations long, was placed around the mean value. The interval ($\bar{X}$ - 2S, $\bar{X}$ + 2S) was divided into 40 equally long classes, and the number of residuals in each class was plotted in a histogram. For comparison a Normal probability distribution function with $\bar{X}$ mean and S standard deviation was plotted in the same diagram.

As the interval of four standard deviations is too short to contain all the residuals, the number of exceeding residuals (NER) is printed together with each histogram. An example of a histogram can be seen in fig. 4.2.

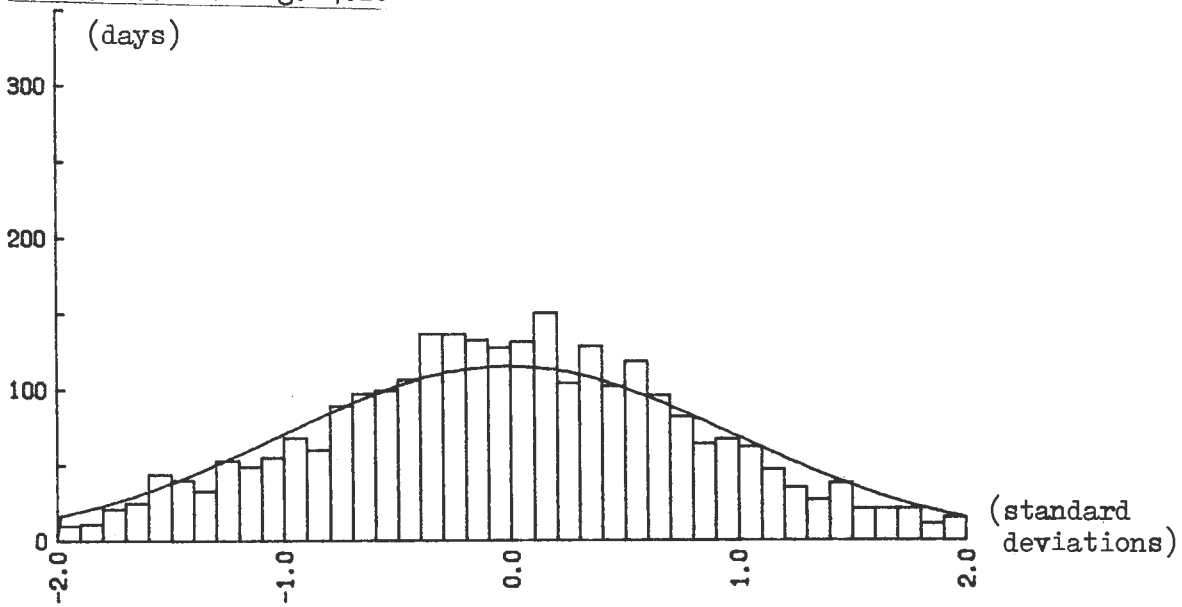

Fig. 4.2 Histogram of the low flow residuals of Kultsjön 62.10.01 - - 76.05.18. Meanvalue = 0.725 (m^3/s). Standard deviation = = 7.07 (m^3/s). NER = 145

All histograms are presented in Appendix A.

A preliminary test was made to study if the mean value of each class of residuals ($\bar{X}$) differed significantly from zero. The simple t-test was used for this purpose. Some apparently significant results were found.

However, the t-test is based on the assumption of independent and $N(\mu, \sigma)$-distributed variables. The assumption of normality is not very critical, but the assumption of independence has to be fullfilled.
As will be shown later, the residuals are not independent. The test was carried out with regard paid to the interdependence, according to Hansen (1971). Thus the quantity $\frac{n}{2\, n_x}$ was interpreted as the equivalent number of independent observations.

Where n_x is defined by:

$$n_x = \int_0^\infty R(\tau)\, d\tau$$

$R(\tau)$ = autocorrelation function of the chosen residuals.

Using the t-test in this way showed no significant deviation from zero on the 5 % level.

However, each class of residuals consists of a number of independent continuous time periods. Regarding this, one could construct a more powerful test.

4.3 Test of normality and independence

Very often in statistical applications the assumptions of mutually independent and normally distributed variables are made.

To test these assumptions on the residuals of different model mechanisms the χ^2-test was used.

$$U = \sum_{i=1}^{k} \frac{(Y_i - np_i)^2}{np_i}$$

where U = test variable,
k = number of test classes,
n = total number of recorded days,
p_i = probability for a normally distributed, stochastic variable to assume a value within class i,
Y_i = observed number of days in class i.

If the assumptions hold, then U is approximately χ^2-distributed with the number of test classes minus three degrees of freedom.

Whenever $np_i < 5$, the test class ,i, was merged with a neighbouring test class, until the probability to fall within test class limits was greater than 5/n. This validity limit is taken from Rudemo, Råde (1970).

Let: $X(t) = Q_r(t) - Q_c(t)$,
where $Q_r(t)$ = observed discharge at day t,
$Q_c(t)$ = computed " " " ".

Table 4.1 χ^2-test made on the residuals. The hypothesis H_o (the X(t):s are mutually uncorrelated with Normal probability distribution function) is tested versus its logical opposite.

Catchment	MSC	Number of observations	Degrees of freedom	Test variable (U)	0.1 % level significance limit of U
Kultsjön	-	4977	38	2210	73
"	snowmelt	1185	"	322	"
"	γ-flow	914	"	166	"
"	low flow	2876	"	99	"
Stadarforsen	-	5273	"	4459	"
"	snowmelt	1156	"	403	"
"	γ-flow	2008	"	420	"
"	low flow	2097	"	354	"

The hypothesis (H_o) that the residuals (X(t):s) are mutually independent with Normal probability distribution function was tested by means of the χ^2-test (tab. 4.1).

The hypothesis had to be rejected on the 0.1 % level.

Although the material was divided into different classes, the hypothesis H_o still did not hold. However, the χ^2-variable (U) was made less by the separation of the different mechanisms. A visual inspection also shows that the residuals are more close to normality in each subclass after the separation. Therefore H_o is, in some sense, more valid after the mechanism separation of the material than before.

Furthermore, the χ^2-test is very sensitive when used on a material built upon many observations. The data may be sufficient in number to show their inconsistency with almost any hypothesis suggested. (Hamon and Hannan, 1963).

The χ^2-test is unfortunately not able to separate the questions of distribution and autocorrelation. As will be shown later, a clearly significant autocorrelation exists in this case. Moreover, mostly the assumption of normally distributed residuals is not very ciritical. Every result below, obtained by relying upon Normal distributions may be considered as an approximation.

4.4 Estimation of the autocorrelation

To estimate the autocorrelation a method described by Jenkins and Watts (1969) was used.

At first the autocovariance was estimated for each continuous period j, when one mechanism was working (see chapter 4.1).

$$\hat{R}_j(\tau) = \frac{1}{N_j - \tau} \sum_{t=t_j}^{N_j-\tau+t_j-1} (X(t+\tau) - \bar{X})(X(t) - \bar{X}),$$

where $\hat{R}_j(\tau)$ = estimated autocovariance of residuals separated by τ days,

$X(t) = Q_r(t) - Q_c(t)$ = residual at time t (m^3/s),

N_j = duration of period j (days),

t_j = the time at which period j started (days from the beginning of the discharge record).

In order to get an overall estimate of the autocovariance the estimates from the different periods with the same mechanism working were brought together as follows.

$$\hat{R}(\tau) = \sum_{\substack{\text{all the} \\ \text{periods } j}} \left(\frac{N_j - \tau}{N_\tau} \hat{R}_j(\tau) \right)$$

where $\hat{R}(\tau)$ = overall estimate of the autocovariance,

$N_\tau = \sum_j (N_j - \tau)$ = the total number of observations of $R(\tau)$ (days).

Finally the autocorrelation was estimated by dividing the estimates of the autocovariance by the estimate of the variance.

When there is less than about 400 observations, one should not rely too much upon the autocorrelation curves, because of the extremely skew probability distribution of the autocovariance.

Kendall and Stuart (1967) actually warned for the use of a correlation coefficient estimate, based on less than 500 observations. However, here we have got autocorrelation estimates at surrounding time intervals too, which gives an indication of the roughness of the estimation procedure. Furthermore the coefficients were estimated from a number of series differing in time.

During series of days with rapidly changing MSC the discharge produced by different physical mechanisms strongly interacts. This may disturb the estimation of the autocorrelation function. (See fig. 4.3, where the estimated autocorrelation exceeds 1.) To avoid this phenomenon a minimum period duration of 5 days was defined. It had to be exceeded without any change in the MSC, if the period was to be used in the autocorrelation estimation procedure. (See fig. 4.4.)

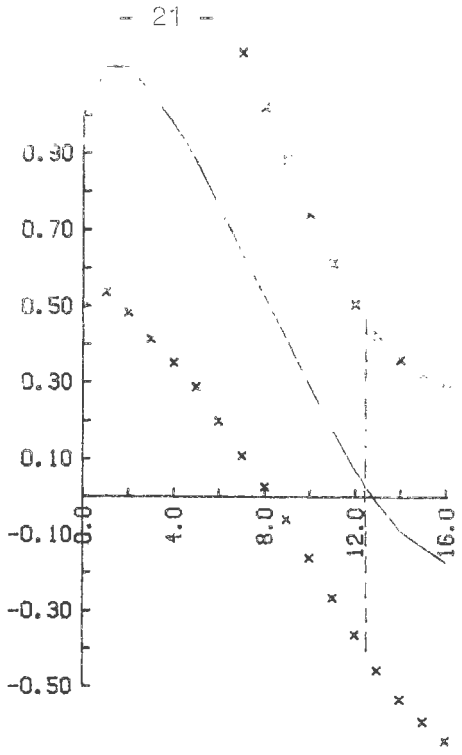

Fig. 4.3 Estimate of the autocorrelation of the model residuals at snowmelt in Stadarforsen 61.10.01 - 76.03.31.
Variance of the residuals = $1.72 \cdot 10^3$ $(m^3/s)^2$.
95 % confidence limits: ×
> 400 observations to the left of the line:
Minimum period duration = 1 day.

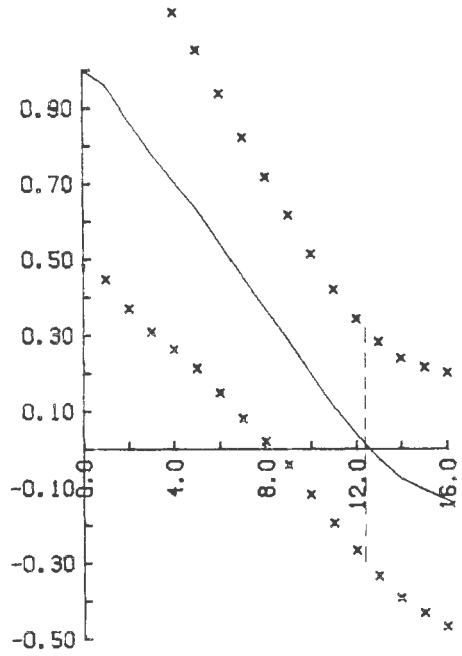

Fig. 4.4 Estimate of the autocorrelation of the model residuals at snowmelt in Stadarforsen 61.10.01 - 76.03.31.
Variance of the residuals = $2.35 \cdot 10^3$ $(m^3/s)^2$.
95 % confidence limits: ×
> 400 observations to the left of the line:
Minimum period duration = 5 days.

4.5 Significance of the autocorrelation

It was considered an important task to determine confidence intervals around the autocorrelation function and especially to tell when it significantly differed from zero.

One method to approach this problem is a significance test developed by Anderson (1941).

The hypothesis that the series is a so called circular series built upon N purely random observations of a normally distributed stochastic variable, is tested. This method was not used because of the difficulty of merging the different significance limits from separate time series, differing in length into an overall significance limit.

Assuming that the residuals are normally distributed and that the estimated mean value is correct, we will obtain:

$$\mathrm{Var}\left[\hat{R}_j(\tau)\right] = \frac{1}{N_j} \sum_{v=-N_j+\tau+1}^{N_j-\tau-1} \left[R_j^2(v) + R_j(v+\tau)\, R_j(v-\tau)\right] \left(1 - \frac{\tau+|v|}{N_j}\right)$$

where $\hat{R}_j(\tau)$ = estimate of the autocovariance function of period j,
N_j = duration of period j (days).

This method is described by Hjorth (1976). Assuming the $\hat{R}_j(\tau)$ of different periods j with the same mechanism working as independent, we get

$$\mathrm{Var}\left[\hat{R}(\tau)\right] = \sum_{\substack{\text{all} \\ \text{periods } j}} \left(\frac{N_j - \tau}{N_\tau}\right)^2 \cdot \mathrm{Var}\left[\hat{R}_j(\tau)\right]$$

Confidence intervals were computed, assuming the $\hat{R}(\tau)$:s to have normal probability distributions. Then the 95 % confidence interval was given in the form:

$$\hat{R}(\tau) \pm 1.96 \cdot \sqrt{\mathrm{Var}\left[\hat{R}(\tau)\right]}$$

When plotted in the autocorrelation graphs all confidence limits had to be divided by $\hat{R}(o)$ in order to get the correct scale. The prodedure led to a slight paradox, the upper confidence limit might exceed one. This is of course impossible, but the autocor-

relation graph should be interpreted as a standardized auto covariance graph. The confidence limits were symmetrically placed on both sides of the autocorrelation estimate.

4.6 Analysis of the autocorrelation

During the beginning of the statistical study the autocorrelation coefficients were believed to contain valuable information.

The kind of intermittent processes described here are not known to be fitted with any standard estimation methods. An aim of this work has been to get unbiased estimations. With increasing number of observations the observed quantity turns more and more normal, and then an unbiased estimation is preferable.

The three MSC are:

1. $M > 0$ (snowmelt),
2. $M \leq 0$ and (S_{uz} or ΔS_{uz}) > 0 (γ-flow),
3. $M \leq 0$ and $S_{uz} = \Delta S_{uz} = 0$ (low flow).

M = snowmelt (mm),
S_{uz} = storage in the upper zone of the model (mm),
ΔS_{uz} = inflow in the " " " " " " .

During snowmelt we have got a clearly significant autocorrelation (see fig. 4.5 and 4.6). This shows us that a large residual during one day will give rise to large residuals during the following days. If, for instance, bad representativeness of the temperature measurements causes false snowmelt one day, the reservoirs of the model are filled up to an improper level. This affects the residuals during the following days.

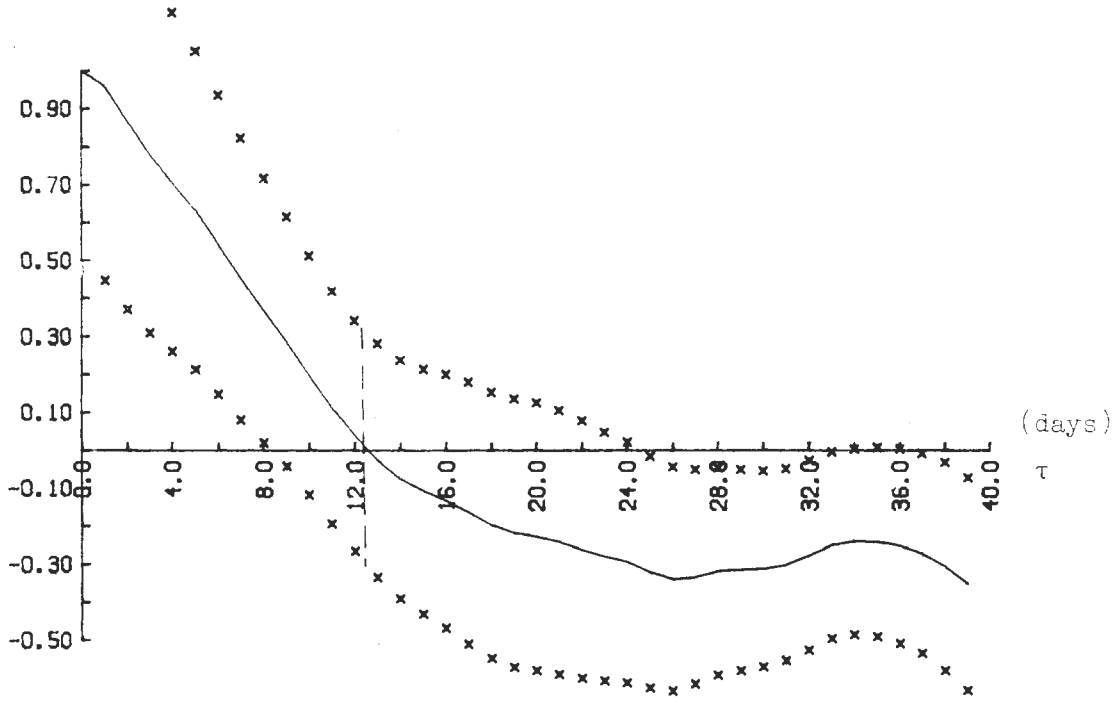

Fig. 4.5 Estimate of the autocorrelation of the residuals of Stadarforsen (snowmelt) 61.10.01 - 76.03.31.
Variance of the residuals = $2.35 \cdot 10^3$ $(m^3/s)^2$.
95 % confidence limits: ×
> 400 observations to the left of the line:

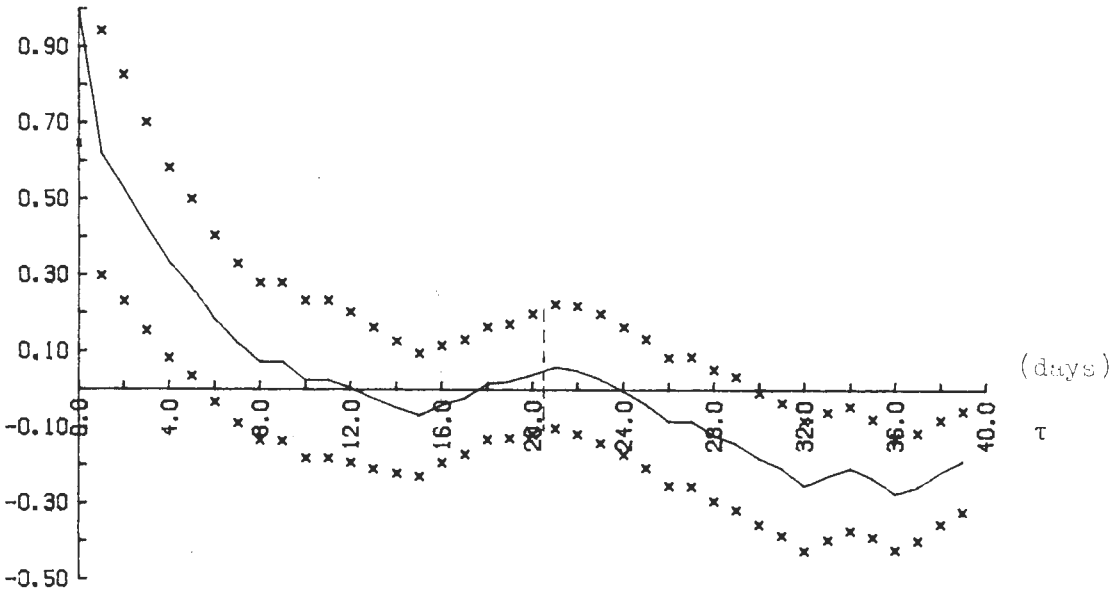

Fig. 4.6 Estimate of the autocorrelation of the residuals of Kultsjön (snowmelt) 62.10.01 - 76.05.18.
Variance of the residuals = $1.13 \cdot 10^3$ $(m^3/s)^2$.
95 % confidence limits: ×
> 400 observations to the left of the line:

The slow decrease of the autocorrelation function of Stadarforsen compared with the one of Kultsjön is presumably due to the facts that:

1. The response in Stadarforsen is more damped.
2. The discharge data of Stadarforsen do not contain the kind of noise that lies on top of the discharge record in Kultsjön, due to the method (Bergström 1976) used when estimating inflow.

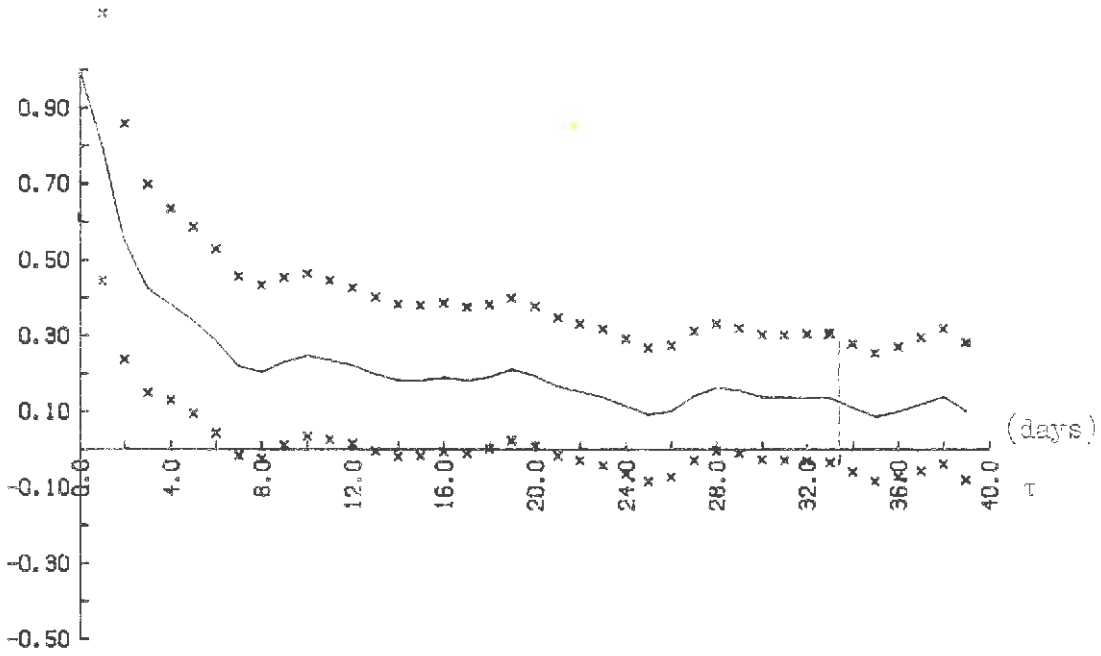

Fig. 4.7 Estimate of the autocorrelation of the residuals of Stadarforsen (Y-flow) 61.10.01 - 76.03.31
Variance of the residuals = 330 $(m^3/s)^2$
95 % confidence limits: ×
> 400 observations to the left of the line:

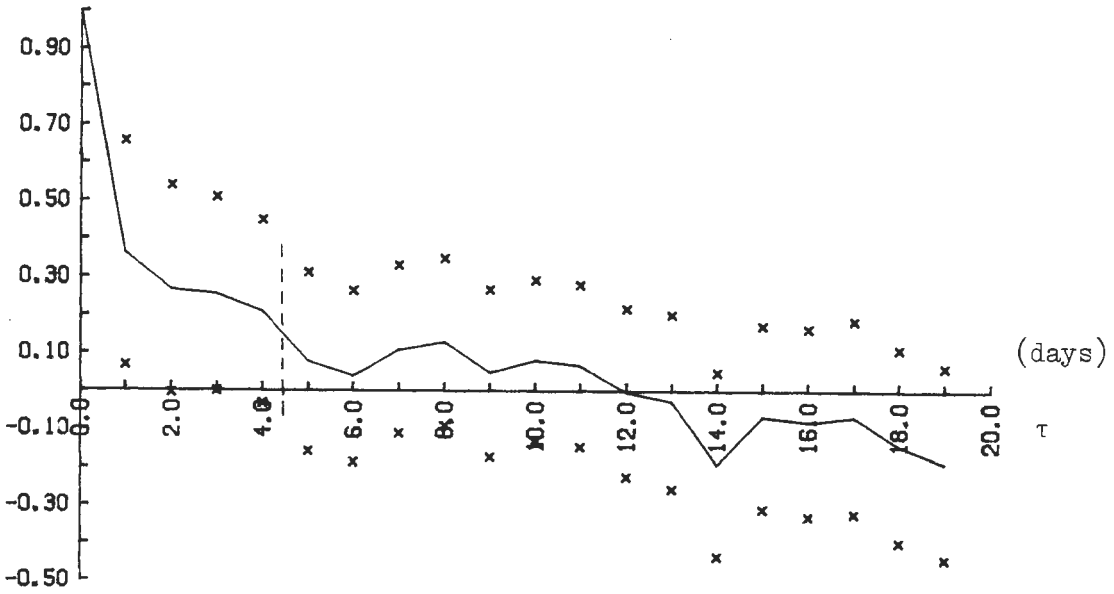

Fig. 4.8 Estimate of the autocorrelation of the residuals of Kultsjön (γ-flow) 62.10.01 - 76.05.18.
Variance of the residuals = 258 · $(m^3/s)^2$
95 % confidence limits: ×
> 400 observations to the left of the line:
Note that due to the small number of observations the maximum argument above is just 19 days.

When the MSC shows γ-flow (fig. 4.7 and 4.8), we have also got a significant autocorrelation. However, it is less than in the former case. A reasonable explanation to this is that the reservoirs may still become filled up to an improper level but not up to the same high level as during snowmelt. This makes the residuals, separated by a shorter time period, independent of each other.

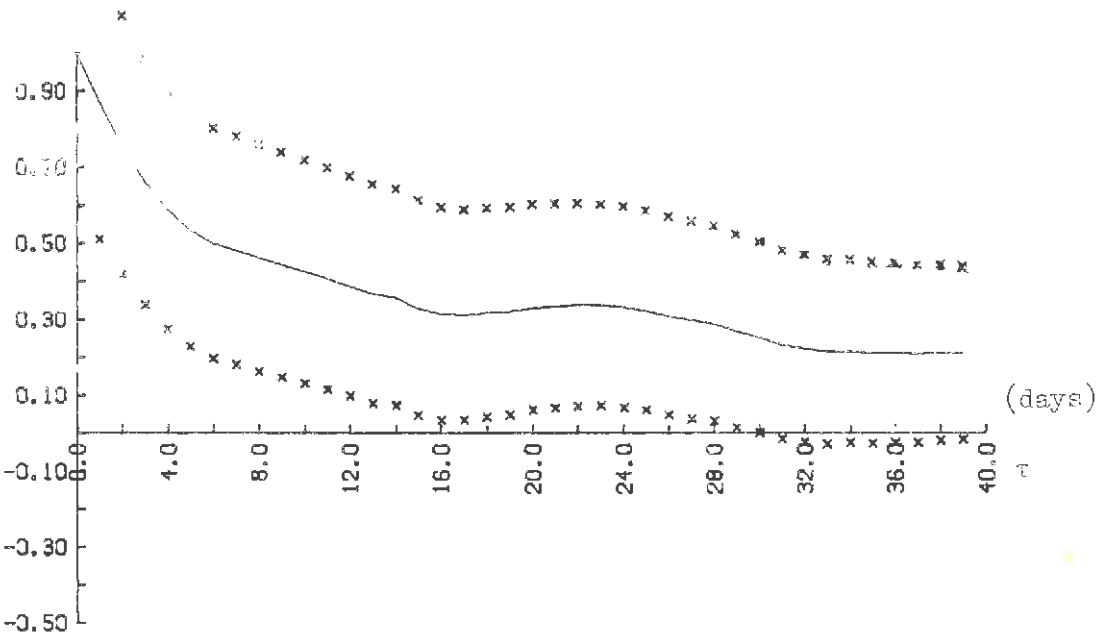

Fig. 4.9 Estimate of the autocorrelation of the residuals of Stadarforsen (low flow) 61.10.01 - 76.03.31.
Variance of the residuals = 19.3 $(m^3/s)^2$.
95 % confidence limits: ×
> 400 observations everywhere.

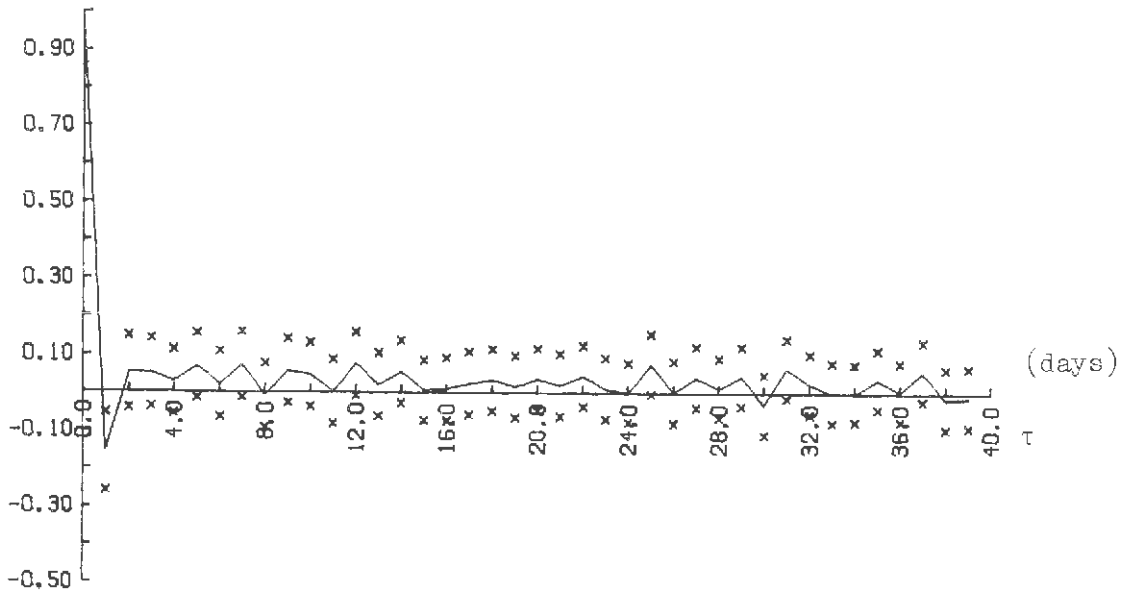

Fig. 4.10 Estimate of the autocorrelation of the residuals of Kultsjön (low flow) 62.10.01 - 76.05.18.
Variance of the residuals = 47.1 · $(m^3/s)^2$
95 % confidence limits: ×
> 400 observations everywhere.

At low flow there are great differences between Stadarforsen and Kultsjön (fig. 4.9 and 4.10).

The noise of the hydrograph of Kultsjön leads to the assumption that any autocorrelation in Kultsjön during low flow is masked by the noise on top of the recorded hydrograph.

In Stadarforsen this is not the case. A nice smooth recession curve gives us large autocorrelation estimations.

If the reservoirs of the model are filled up to an improper level during or before the winter recession, this will cause a very persistant series of residuals.

5. A STUDY OF RESPONSE SURFACES OF CRITERIA OF FIT

5.1 Criteria of fit

Nash and Sutcliffe (1970) defined the R^2-criterion of fit as the efficiency of the model.

$$R^2 = \frac{\sum_t (Q_r(t) - \overline{Q}_r)^2 - \sum_t (Q_r(t) - Q_c(t))^2}{\sum_t (Q_r(t) - \overline{Q}_r)^2}$$

where $Q_r(t)$ = observed discharge at time t (m^3/s),
$Q_c(t)$ = computed " " " " " ,
$\overline{Q}_r$ = arithmetic mean of $Q_r(t)$.

The R^2-criterion of fit is widely spred and it has a relative character, which makes it attractive when comparing the fit of different models, different time periods or different catchments.

These comparisons should not be made between hydrographs that differ too much, because of the phenomenon illustrated in fig. 5.1 and 5.2, which could be due to one or both of the following explanations.

1. Inevitable errors of roughly constant size cause the R^2-criterion to give high values when applied to hydrographs with high initial variance and vice versa.
2. The calibration of the model and the model itself favour fit during periods with high initial variance, and so the relative fit is bound to be worse during periods with low initial variance.

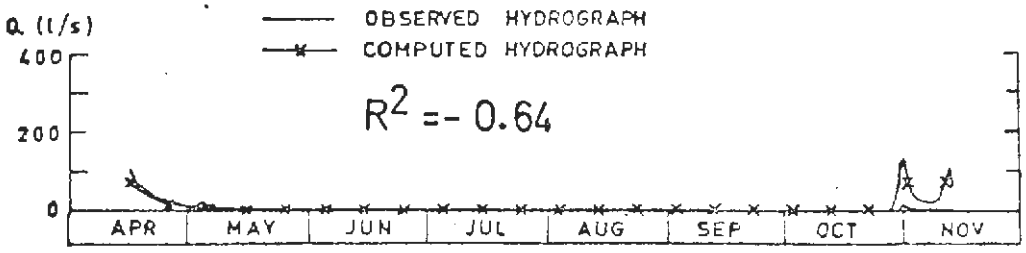

Fig. 5.1. Low R^2-value as a result of low initial variance (Stabby, 1959). (From Bergström, 1976.)

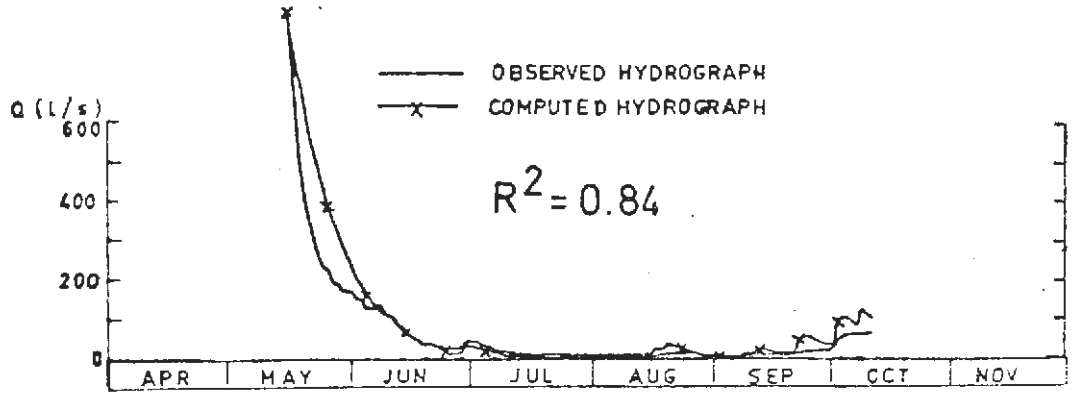

Fig. 5.2. High R^2-value as a result of high initial variance (L. Tivsjön, 1968). (From Bergström, 1976.)

The initial variance from a sample of n observations is defined by:

$$F_o^2 = \frac{1}{n-1} \sum_{t=1}^{n} (Q_r(t) - \bar{Q}_r)^2.$$

The R^2-criterion was computed for each class and also for the material as a whole. The obtained criteria are called:

R_1^2 during snowmelt,

R_2^2 during rain or recession succeeding rain or snowmelt (γ-flow),

R_3^2 during dry summer or winter recession (low flow),

R_w^2 for the material as a whole,

$R_{sum} = R_1^2 + R_2^2 + R_3^2$.

Up till today the R_w^2-criterion has been used as a help during the calibration by visual inspection of the hydrograph.

Let us assume that the R^2-criteria of different physical processes do give a more accurate measure of the goodness of fit between the computed and the recorded hydrograph. Then the problem of merging the three criteria into one arises. One possibility of doing this is simply to add up the three criteria, thus achieving the R_{sum}-criterion.

5.2 Basic assumptions and observations

The MSC gives different classifications of the material at different parameter settings. This sometimes made the R^2-criteria vary unexpectedly (especially the R_3^2-criterion). If a couple of days are moved to the low flow class from the other classes, this will probably make the initial variance (F_o^2) of the low flow class greater, but it might possibly not influence the sum $\sum_t (Q_r(t) - Q_c(t))$ to the same extent. Thus, the R_3^2-criterion will grow perhaps without any visible change in the hydrograph, a phenomenon similar to the one illustrated in fig. 5.1 and 5.2.

The HBV-model has always been calibrated by visual inspection of the computed and recorded hydrographs. This means that a considerable skill in parameter setting has been obtained during the years. For example, recently on the first try when calibrating the HBV-model for a new catchment the R_w^2-value of the four year calibration period was greater than 0.8.

This implies that a fairly good parameter setting could be obtained by a qualified guess based on experience from other applications. It is likely that an automatic parameter optimization routine would accomplish this too.

This assumption made the work easier, while only the region around the optimum parameter setting had to be examined. The subjectively found optimum (tab. 5.1) was used as the actual one, and the parameters were varied around this central point.

Table 5.1 Original settings of the free parameters of the HBV-model.

Parameter	Kultsjön	Stadarforsen
P_{corr}	1.330	1.136
T_o (^oC)	0.5	0.0
C_{sf}	1.23	0.90
C_o (mm/(^oC · day))	3.2	2.0
C_{wh}	0.05	0.05
S_b (mm)	0.0	0.0
C_{rfr}	1.0	1.0
Fc (mm)	150	150
L_p (mm)	150	150
β	3.0	1.5
K_o (1/(s · mm))	0	12500
K_1 (1/(s · mm))	4000	3500
K_2 (1/(s · mm))	300	350
L_{uz} (mm)	∞	15
C_{perc} (mm/day)	1.3	1.0
B_{max} (days)	2.0	6.0
C_{route} (day · s/m^3)	0.00103	0.00000

Note that K_o in Kultsjön is zero. That version of the HBV-model is older than the one used in Stadarforsen. It is occasionally used when the catchment behaviour is determined to be sufficiently simple. Because there were no initial values of K_o and L_{uz}, a variation of these parameters in Kultsjön was avoided.

During the original subjective calibration 8-year periods were used, but due to the limited capacity of the computer only 4-year periods were used in the study of the response of the R^2-criteria. This limits the value of the comparisons between the model behaviour of the original parameter setting and the test settings of this study. The periods studied are in Stadarforsen 1965-10.01--1969-09-30 and in Kultsjön 1962-10-01 --1966-09-30.

Two, sometimes three, parameters were varied simultaneously, and the R^2-criteria were computed at the different parameter settings. This resulted in tables and "three-dimensional" diagrams of iso-R^2 graphs. The R^2-curves were only drawn around the optimum point.

If there was a substantial difference between the R^2-values at the optimum and at the original parameter setting, the computed hydrograph corresponding to the optimum values of the parameters was plotted. These hydrographs were later judged by the model calibraters in order to estimate the goodness of fit at the new parameter settings.

R_1^2

K_2 / C_{perc}	100	200	300	400	500	600	700	800	900	1000
9	.704	.709	.710	.709	.707	.	.	.	.	.
12	.707	.714	.716	.715	.713	.	.	.	.	.
15	.709	.718	.721	.720	.719	.	.	.	.	.
18	.708	.720	.724	.725	.724	.	.	.	.	.
21	.706	.720	.727	.728	.728	.	.	.	.	.
24	.701	.719	.727	.730	.730	.729	.727	.725	.723	.721
27	.694	.715	.727	.731	.732	.731	.730	.728	.726	.724
30	.685	.711	.725	.731	.733	.733	.732	.730	.728	.726
33	.674	.704	.722	.730	.734	.734	.733	.732	.730	.728
36	.	.	.	.	.	.735	.734	.733	.732	.730

R_2^2

K_2 / C_{perc}	100	200	300	400	500	600	700	800	900	1000
9	.538	.543	.538	.530	.522	.	.	.	.	.
12	.548	.554	.547	.539	.530	.	.	.	.	.
15	.551	.559	.552	.544	.536	.	.	.	.	.
18	.555	.566	.558	.550	.542	.	.	.	.	.
21	.557	.569	.560	.552	.544	.	.	.	.	.
24	.551	.566	.559	.551	.545	.540	.534	.528	.520	.512
27	.552	.567	.558	.551	.546	.542	.537	.531	.525	.518
30	.543	.559	.549	.543	.540	.537	.534	.530	.525	.519
33	.533	.549	.539	.533	.532	.532	.531	.529	.525	.520
36	.	.	.	.	.	.524	.524	.524	.520	.519

Fig. 5.3 The response of the R^2-criteria to K_2 (1/(s · mm)) and C_{perc} (10^{-1} mm/day) at Kultsjön. (See chapter 5.3; 5.3.1)

R_3^2

K_2 / C_{perc}	100	200	300	400	500	600	700	800	900	1000
9	.145	.233	.254	.248	.232	.	.	.	.	.
12	.161	.274	.306	.306	.293	.	.	.	.	.
15	.151	.286	.328	.332	.323	.	.	.	.	.
18	.141	.292	.344	.355	.351	.	.	.	.	.
21	.113	.285	.347	.365	.366	.	.	.	.	.
24	.079	.265	.333	.354	.358	.354	.347	.337	.327	.316
27	.067	.260	.332	.358	.367	.368	.364	.358	.350	.341
30	.024	.229	.307	.337	.350	.353	.352	.348	.341	.334
33	.009	.220	.300	.334	.349	.356	.358	.356	.358	.347
36	.	.	.	.	.	.336	.341	.341	.339	.335

R_w^2

K_2 / C_{perc}	100	200	300	400	500	600	700	800	900	1000
9	.777	.783	.783	.782	.780	.	.	.	.	.
12	.780	.788	.789	.788	.786	.	.	.	.	.
15	.781	.790	.792	.792	.790	.	.	.	.	.
18	.780	.791	.795	.795	.793	.	.	.	.	.
21	.777	.791	.796	.796	.795	.	.	.	.	.
24	.772	.789	.795	.797	.796	.795	.793	.791	.789	.787
27	.766	.786	.794	.796	.797	.796	.794	.793	.792	.790
30	.759	.781	.791	.795	.796	.796	.795	.793	.792	.790
33	.751	.776	.787	.792	.794	.795	.795	.794	.792	.791
36	.	.	.	.	.	.794	.794	.793	.792	.791

Fig. 5.3

5.3 The response surfaces of criteria of fit and test plottings of Kultsjön

For the interpretation of the model parameters see chapter 3 and for the initial values of the parameters see tab. 5.1.

5.3.1 The response of the R^2-criteria to K_2 and C_{perc}

The variation of each R^2-criterion was computed when altering K_2 and C_{perc}. Since these parameters have their greatest influence on low flow, the R_3^2-criterion was considered most important. In fig. 5.3 the R_3^2-criterion indicates that C_{perc} and K_2 should be increased. The irregular shape of the R_3^2-response surface is due to the variable classification by the MSC (chapter 5.2).

An increase in C_{perc} will have the effect of increasing the overall flow during low flow. It will also cause a shorter duration of the peak flows. An increase in K_2 will accelerate the low flow recession. A test plotting was made at:

K_2 = 600 l/s · mm,
C_{perc} = 2.7 mm/day,

which is the optimum point during low flow.

The new hydrograph was considered to be somewhat better than the old one.

5.3.2 The response of the R^2-criteria to K_1, B_{max} and C_{route}

The R_2^2-criterion in fig. 5.4 obviously points towards a decrease in K_1 and C_{route}. A decrease in K_1 will make the hydrograph more damped and will also cause a considerable number of days to move from the low flow class to the Y-flow class. The latter is the reason why we get such odd information from the R_3^2-criterion here.

C_{route}, too, affects the variance of the hydrograph. A low C_{route} value will damp the discharge peaks, while a high value will make the hydrograph vary in a more rapid way.

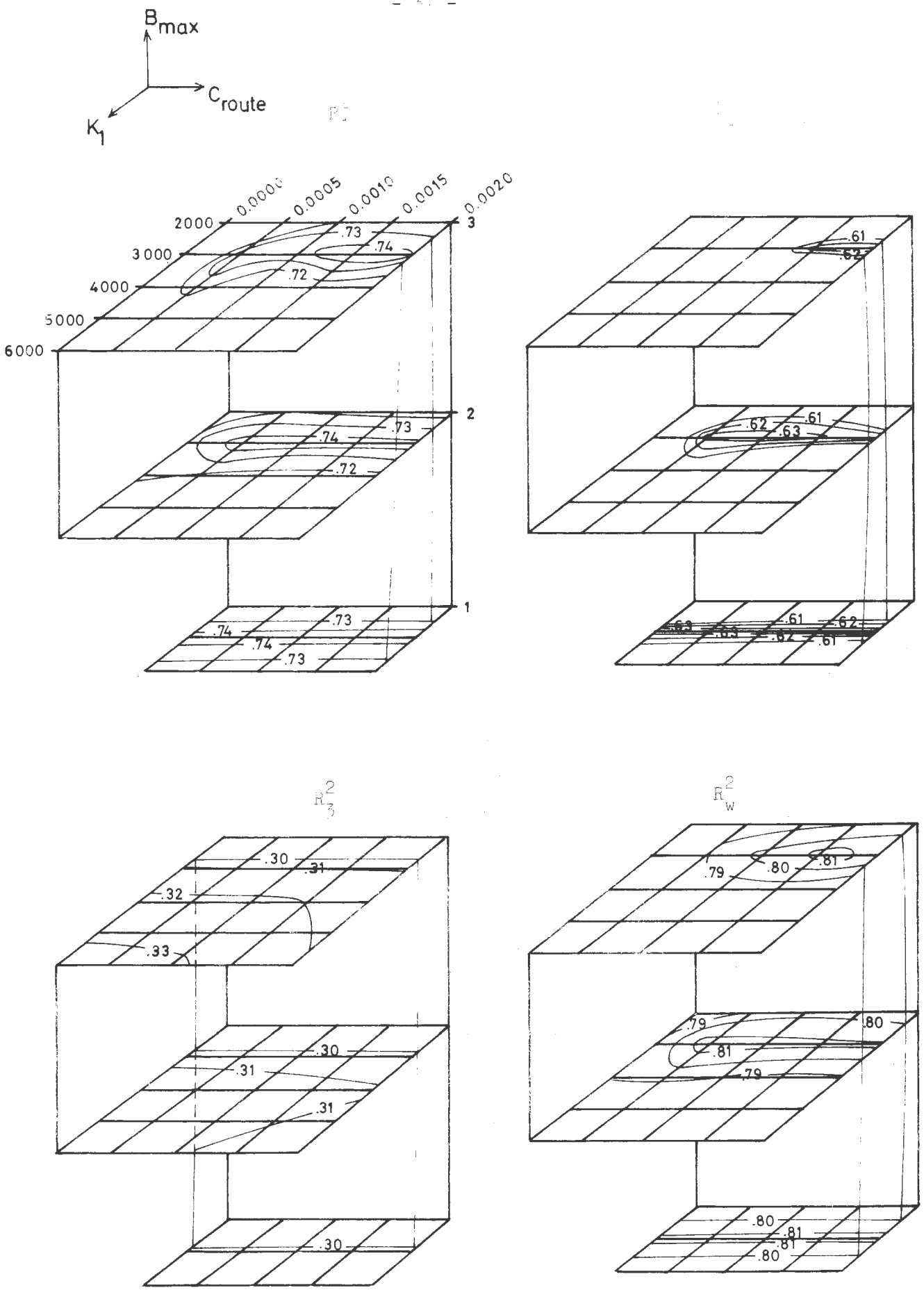

Fig. 5.4 The response of the R^2-criteria to K_1 (1/(s · mm)), B_{max} (days) and C_{route} (day · s/m^3) at Kultsjön.

(See chapter 5.3; 5.3.2)

A test plotting was made at:

K_1 = 3000 l/s · mm,
C_{route} = 0.001 day/(m^3/s),
P_{max} = 2 days.

Here the model demonstrates an unability to move rapidly between high and medium flows by consistently underestimating high flows. This underestimation was considered serious and caused the calibraters to judge the plotting to be not as good as the original one.

The lack of a K_o parameter is likely to be the cause of this damped behaviour of the model, since one further storage discharge parameter would increase the slope of the recession.

5.3.3 The response of the R^2-criteria to Fc, L_p/Fc and β

The parameters varied in fig. 5.5 affect the evaporation. They also affect the level of the flow peaks succeeding dry periods.

The optimum of the R_w^2-cirterion seems to be:

Fc = 200 mm,
L_p/Fc = 0.6 $\rightarrow L_p$ = 120 mm,
β = 2 or 4.

Two test plottings are made, one at β = 2 and one at β = 4. They do not differ much from each other, but they differ from the original plotting. The decrease in the L_p/Fc ratio causes an increase in the evaporation. This leads to an underestimation of the high flow peaks of summer. Thus, the test plottings were inferior to the original one. The medium and low summer flows are perhaps a bit better on the test plottings than on the original one. Again the lack of a third storage discharge parameter (K_o) is obvious.

Fig. 5.5 (See next page).
The response of the R^2-criteria to Fc, L_p/Fc and β at Kultsjön.

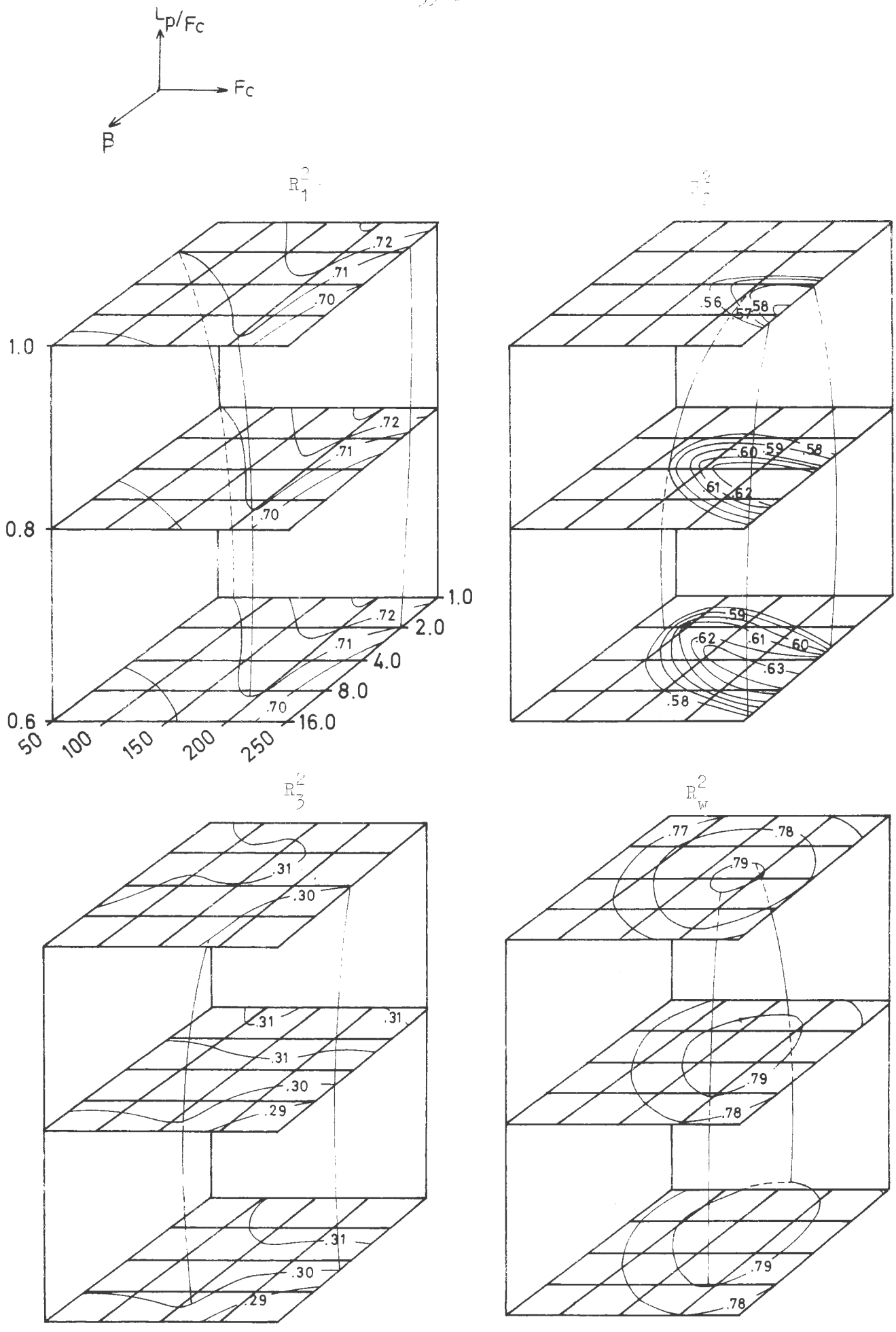

Fig. 5.5 (See chapter 5.3; 5.3.3)

5.3.4 The response of the R^2-criteria to C_{sf} and β

β and C_{sf} both affect the losses between precipitation and runoff. The differences between the optima of these response surfaces and the R^2-values of the original parameter setting was small and no test plotting was made.

R_1^2

C_{sf} \ β	1.	2.	4.	8.	16.
1.0	.699	.690	.671	.651	.637
1.1	.737	.729	.715	.700	.689
1.2	.737	.730	.722	.713	.706
1.3	.686	.680	.678	.675	.672
1.4	.607	.603	.608	.610	.609

R_3^2

C_{sf} \ β	1.	2.	4.	8.	16.
1.0	.317	.323	.319	.315	.306
1.1	.313	.319	.315	.309	.305
1.2	.308	.315	.312	.310	.305
1.3	.303	.301	.308	.304	.302
1.4	.299	.297	.305	.301	.299

R_2^2

C_{sf} \ β	1.	2.	4.	8.	16.
1.0	.396	.540	.561	.485	.359
1.1	.368	.533	.571	.501	.377
1.2	.334	.513	.565	.499	.375
1.3	.317	.499	.555	.487	.359
1.4	.303	.483	.538	.466	.338

R_w^2

C_{sf} \ β	1.	2.	4.	8.	16.
1.0	.765	.774	.766	.748	.728
1.1	.783	.794	.790	.776	.758
1.2	.781	.793	.794	.783	.768
1.3	.753	.767	.771	.763	.750
1.4	.708	.722	.730	.724	.712

Fig. 5.6 The response of the R^2-criteria to C_{sf} and β at Kultsjön.

R_1^2

T_o \ C_o	1.4	1.7	2.0	2.3	2.6	2.9	3.2	3.5	3.8
-1.0	.670	.714	.672	.598	.	.	.	.	.
-0.5	.612	.709	.750	.726	.675	.612	.539	.466	.399
0.0	.468	.610	.707	.745	.744	.716	.668	.618	.558
0.5	.221	.425	.532	.633	.689	.706	.717	.697	.665
1.0	.	.	.	.	.473	.546	.582	.608	.620
1.5	.	.	.	.	.211	.251	.307	.357	.395

R_2^2

T_o \ C_o	1.4	1.7	2.0	2.3	2.6	2.9	3.2	3.5	3.8
-1.0	.513	.482	.553	.567	.	.	.	.	.
-0.5	.449	.478	.492	.551	.556	.555	.515	.492	.446
0.0	.292	.419	.446	.503	.545	.582	.579	.549	.517
0.5	.570	.318	.450	.447	.492	.540	.554	.571	.585
1.0	.	.	.	.	.433	.452	.499	.511	.553
1.5	.	.	.	.	.344	.398	.408	.467	.500

R_3^2

T_o \ C_o	1.4	1.7	2.0	2.3	2.6	2.9	3.2	3.5	3.8
-1.0	.277	.299	.317	.325	.	.	.	.	.
-0.5	.273	.285	.303	.320	.332	.336	.337	.329	.314
0.0	.263	.278	.287	.302	.316	.329	.336	.337	.338
0.5	.243	.265	.274	.281	.292	.300	.313	.321	.323
1.0	.	.	.	.	.286	.292	.305	.311	.322
1.5	.	.	.	.	.274	.282	.285	.288	.295

R_w^2

T_o \ C_o	1.4	1.7	2.0	2.3	2.6	2.9	3.2	3.5	3.8
-1.0	.745	.765	.746	.704	.	.	.	.	.
-0.5	.706	.769	.791	.784	.756	.717	.669	.620	.571
0.0	.610	.708	.768	.795	.800	.788	.763	.733	.697
0.5	.471	.595	.673	.729	.767	.783	.790	.784	.766
1.0	.	.	.	.	.656	.697	.724	.741	.753
1.5	.	.	.	.	.498	.540	.575	.609	.636

Fig. 5.7 The response of the R^2-criteria to T_o and C_o (mm/(°C · day)) at Kultsjön. (See chapter 5.3; 5.3.5)

5.3.5 The response of the R^2-criteria to T_o and C_o

T_o affects the starts of the melt periods, while C_o affects the overall melt ratio (fig. 5.7).

A test plotting was made at:

$T_o = 0.0\ ^oC$,
$C_o = 2.6$ mm/(^oC · day).

The test plotting showed out to be inferior to the original plotting. There seems to be no way to make the model fit the recorded hydrograph on both peak flow and medium flow. One further degree of freedom is needed.

5.3.6 The response of the R^2-criteria to C_{wh} and C_{rfr}

The parameters C_{wh} and C_{rfr} influence the behaviour of the model, when a melt period is restarted after a short interruption by too low temperatures. The use of the C_{rfr} parameter started during this study of the HBV-model, and the value of having such a parameter was questioned.

As the response surfaces (fig. 5.8) show, C_{rfr} does not affect the R^2-criteria very much, so the C_{rfr} parameter seems to be of no use here.

The optimum value of C_{wh} is obviously 0.05. No test plotting was made, since the optimum values of C_{wh} and C_{rfr} do not deviate from the original ones.

R_1^2

C_{rfr} / C_{wh}	0.00	0.05	0.10	0.20	0.40	1.00
0.00	.701	.701	.701	.701	.701	.
0.05	.709	.704	.708	.711	.715	.717
0.10	.714	.686	.682	.683	.677	.
0.15	.709	.665	.660	.661	.644	.
0.20	.700	.635	.630	.628	.604	.

R_2^2

C_{rfr} / C_{wh}	0.00	0.05	0.10	0.20	0.40	1.00
0.00	.566	.566	.566	.566	.566	.
0.05	.566	.562	.559	.556	.556	.551
0.10	.564	.561	.557	.553	.550	.
0.15	.562	.555	.551	.547	.543	.
0.20	.556	.547	.543	.540	.534	.

R_3^2

C_{rfr} / C_{wh}	0.00	0.05	0.10	0.20	0.40	1.00
0.00	.326	.326	.326	.326	.326	.
0.05	.328	.318	.317	.315	.314	.313
0.10	.323	.306	.300	.298	.295	.
0.15	.320	.292	.289	.286	.286	.
0.20	.313	.287	.284	.283	.281	.

R_w^2

C_{rfr} / C_{wh}	0.00	0.05	0.10	0.20	0.40	1.00
0.00	.770	.770	.770	.770	.770	.
0.05	.778	.783	.785	.787	.789	.790
0.10	.784	.781	.780	.781	.778	.
0.15	.785	.773	.771	.772	.765	.
0.20	.783	.761	.760	.759	.748	.

Fig. 5.8 The response of the R^2-criteria to C_w and C_{rfr} at Hultsjön. (See chapter 5.3; 5.3.6)

R_1^2

K_2	100	200	300	400	500
C_{perc}					
0.0	.864	.866	.867	.868	.869
0.5	.886	.886	.886	.886	.886
1.0	.893	.895	.896	.895	.895
1.5	.887	.893	.894	.894	.894
2.0	.864	.877	.880	.881	.881

R_2^2

K_2	100	200	300	400	500
C_{perc}					
0.0	.571	.576	.577	.574	.568
0.5	.693	.706	.711	.711	.706
1.0	.677	.734	.751	.756	.755
1.5	.623	.717	.747	.758	.759
2.0	.560	.676	.713	.726	.727

R_3^2

K_2	100	200	300	400	500
C_{perc}					
0.0	.000	.000	.000	.000	.000
0.5	-1.470	-.381	-.301	-.495	-.774
1.0	-.227	.468	.649	.636	.530
1.5	-.101	.332	.500	.545	.521
2.0	-.043	.228	.365	.423	.431

R_w^2

K_2	100	200	300	400	500
C_{perc}					
0.0	.872	.873	.874	.874	.874
0.5	.902	.905	.905	.905	.904
1.0	.905	.914	.917	.917	.916
1.5	.895	.910	.914	.915	.914
2.0	.872	.892	.898	.900	.901

Fig. 5.: The response of the R^2-criteria to K_2 (l/(s · mm)) and C_{perc} (1/day) at Stadarforse. (See chapter 5.4; 5.4.1)

5.4 The response surfaces of criteria of fit and test plottings of Stadarforsen

In Stadarforsen runoff data of better quality than in Kultsjön were available. For the interpretation of the model parameters see chapter 3 and for the initial values of the parameters see tab. 5.1.

5.4.1 The response of the R^2-criteria to K_2 and C_{perc}

There is no difference between the optimum parameter setting here (fig. 5.9) and the original one, and so no test plotting was made.

There has been difficulties in finding the optimum setting of K_2 and C_{perc}. But note that there is a clearly observable optimum in the dry summer and winter recession class here.

5.4.2 The response of the R^2-criteria to K_1, C_{route} and B_{max}

The original parameter setting is within the limits of acceptance in fig. 5.10. The R^2_w-criterion does not vary much when B_{max} is varied in a region around the original parameter setting. To study this apparent independence a test plotting was made at:

K_1 = 3 500 l/s · mm,
C_{route} = 0 day/(m^3/s),
B_{max} = 5 days,

where there is a small improvement of the R^2_w-criterion but the new plotting had approximately the same fit as the original one, as judged by the calibrators.

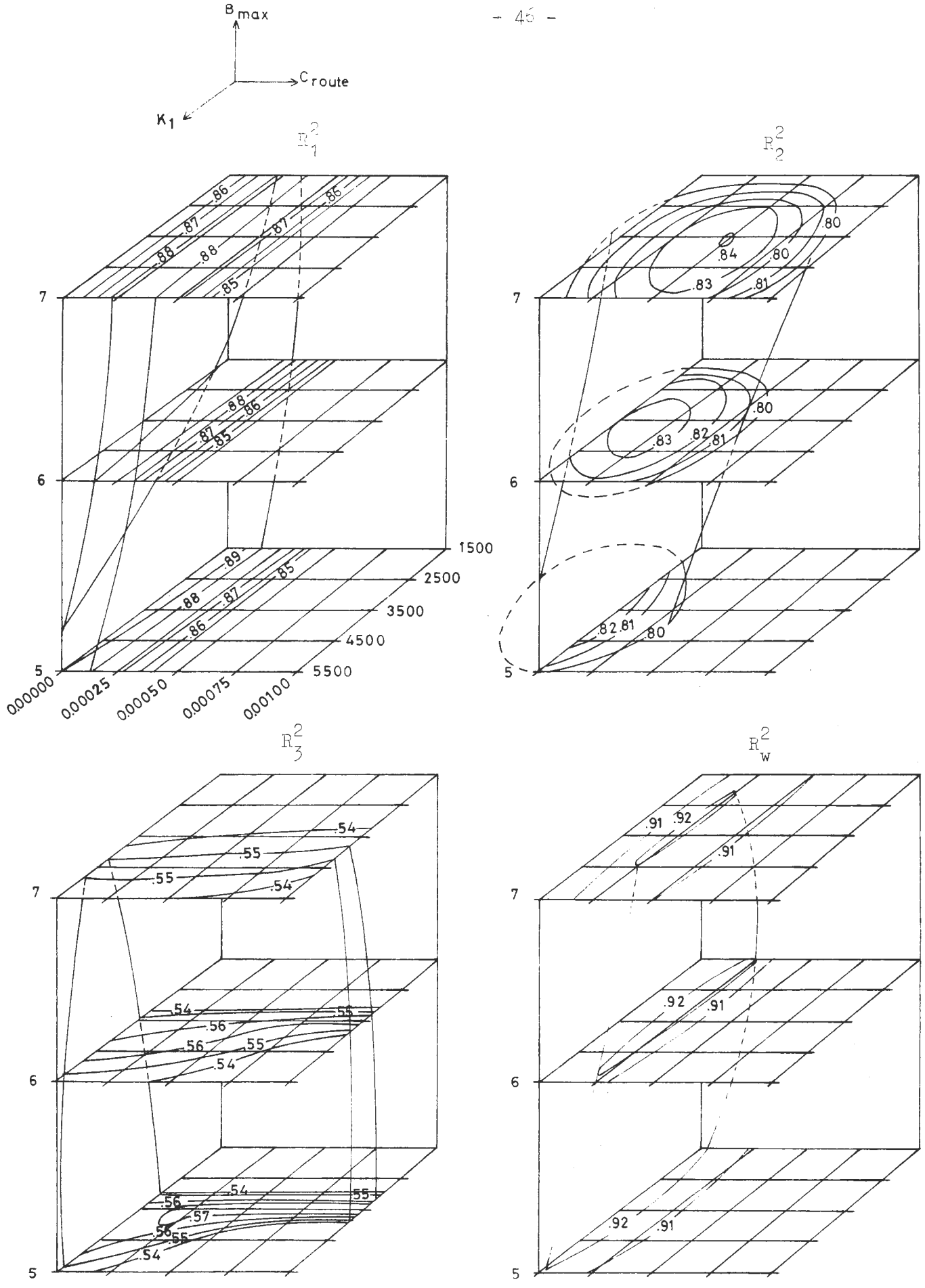

Fig. 5.10 The response of the R^2-criteria to K_1 (1/(s · mm)), C_{route} (day · s/m^3) and B_{max} (days) at Stadarforsen. (See chapter 5.4; 5.4.2)

R_1^2

K_o / L_{uz}	7500	10000	12500	15000	17500	20000	22500	25000
5	.796	.850	.870	.875	.870	.	.	.
10	.794	.851	.875	.884	.883	.	.	.
15	.790	.850	.879	.891	.894	.	.	.
20	.783	.846	.878	.894	.901	.901	.899	.894
25	.774	.838	.873	.892	.901	.905	.905	.903
30	.	.	.	.	.	.903	.906	.906

R_2^2

K_o / L_{uz}	7500	10000	12500	15000	17500	20000	22500	25000
5	.794	.752	.692	.628	.567	.	.	.
10	.819	.809	.782	.753	.721	.	.	.
15	.828	.836	.831	.819	.806	.	.	.
20	.820	.841	.847	.848	.846	.842	.837	.832
25	.798	.824	.837	.845	.850	.853	.855	.856
30	.	.	.	.	.	.833	.837	.841

R_3^2

K_o / L_{uz}	7500	10000	12500	15000	17500	20000	22500	25000
5	.566	.537	.508	.487	.453	.	.	.
10	.551	.543	.544	.533	.524	.	.	.
15	.511	.545	.550	.549	.549	.	.	.
20	.496	.504	.505	.505	.512	.514	.518	.519
25	.483	.492	.496	.496	.496	.504	.504	.504
30	.	.	.	.	.	.491	.492	.492

R_w^2

K_o / L_{uz}	7500	10000	12500	15000	17500	20000	22500	25000
5	.867	.895	.902	.900	.894	.	.	.
10	.867	.899	.912	.914	.912	.	.	.
15	.865	.900	.917	.923	.924	.	.	.
20	.861	.898	.918	.927	.930	.931	.929	.926
25	.855	.893	.914	.925	.931	.933	.934	.932
30	.	.	.	.	.	.931	.933	.933

Fig. 5.11 The response of the R^2-criteria to K_o (1/(s · mm)) and L_{uz} (mm) at Stadarforsen. (See chapter 5.4; 5.4.

5.4.3 The response of the R^2-criteria to K_o and L_{uz}

K_o affects the top flow recession rate and L_{uz} the level, at which this recession rate is activated. A great improvement of the R^2-criteria can be seen here. It is only the R^2_3-criterion that is not improved when increasing K_o and L_{uz}. (Fig. 5.11).

A test plotting was made at:

K_o = 22 500 l/s · mm,
L_{uz} = 25 mm.

The plotting corresponds to the information available through the R^2-criteria. The result is a better overall fit, especially at high flows but perhaps there is some deterioration at low flow.

5.4.4 The response of the R^2-criteria to K_o and K_1

In fig. 5.12 we have got an example of how the snowmelt (R^2_1) class practically governs the R^2_w-criterion. A test plotting was made at the optimum of the R^2_w-criterion.

K_o = 16 500 l/s · mm,
K_1 = 3 500 l/s · mm.

It showed out to be somewhat inferior to the original plotting. The difference, however, was considered to be of minor importance.

Fig. 5.12 The response of the R^2-criteria to K_o (l/(s · mm)) and K_1 (l/(s · mm)) at Stadarforsen. (See next page)

R_1^2

K_1 \ K_o	8500	10500	12500	14500	16500	18500	20500
1500	.820	.860	.851	.891	.894	.	.
2500	.819	.858	.879	.890	.894	.	.
3500	.819	.857	.879	.889	.893	.893	.890
4500	.820	.857	.878	.889	.893	.893	.890
5500	.821	.857	.878	.888	.892	.	.

R_2^2

K_1 \ K_o	8500	10500	12500	14500	16500	18500	20500
1500	.812	.802	.785	.765	.744	.	.
2500	.837	.834	.823	.809	.794	.	.
3500	.835	.836	.831	.822	.811	.800	.789
4500	.824	.827	.826	.820	.812	.803	.794
5500	.810	.816	.813	.809	.802	.	.

R_3^2

K_1 \ K_o	8500	10500	12500	14500	16500	18500	20500
1500	.380	.414	.440	.458	.472	.	.
2500	.452	.466	.475	.479	.478	.	.
3500	.528	.543	.550	.549	.549	.550	.551
4500	.581	.577	.563	.560	.557	.555	.552
5500	.564	.549	.547	.542	.539	.	.

R_w^2

K_1 \ K_o	8500	10500	12500	14500	16500	18500	20500
1500	.882	.904	.916	.920	.921	.	.
2500	.883	.905	.917	.922	.923	.	.
3500	.883	.905	.917	.922	.924	.923	.921
4500	.882	.904	.916	.922	.924	.923	.921
5500	.882	.903	.914	.920	.922	.	.

Fig. 5.12

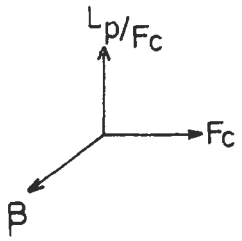

R_1^2

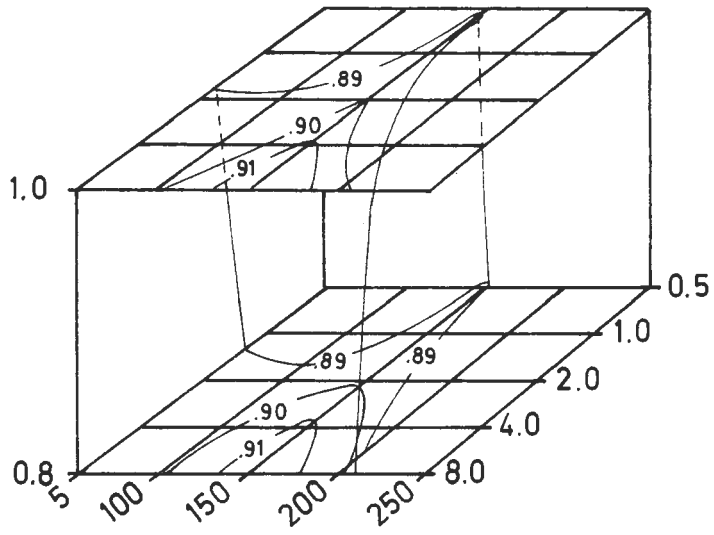

R_2^2

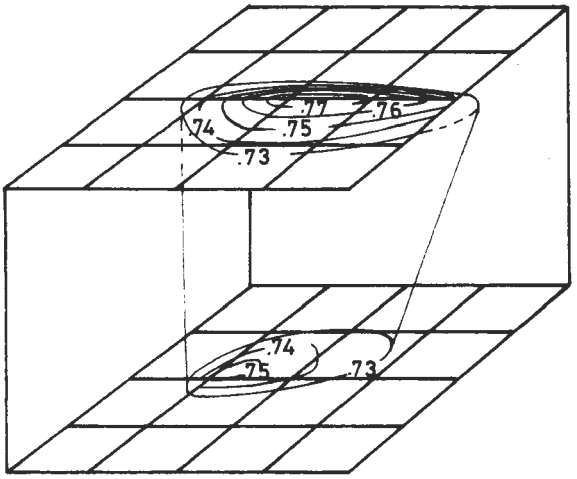

R_3^2

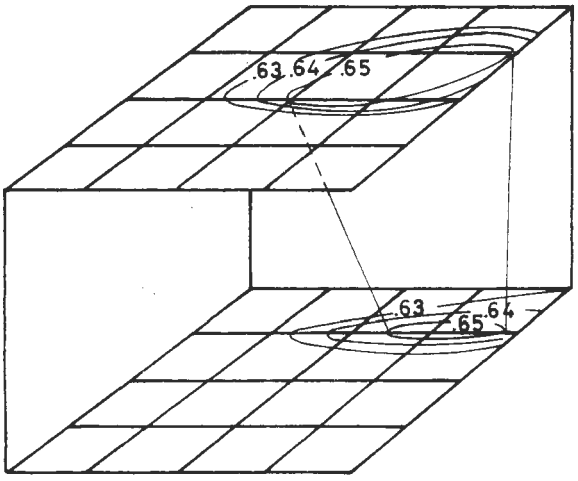

R_w^2

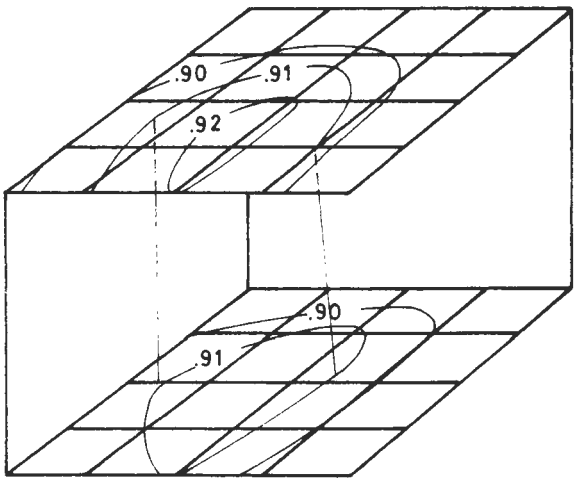

Fig. 5.13 The response of the R^2-criteria to Fc (mm), L_p/Fc and β at Stadarforsen. (See chapter 5.4; 5.4.5)

R_1^2

β / C_{sf}	0.5	1.0	2.0	4.0	8.0
0.80	.888	.893	.905	.912	.908
0.85	.888	.892	.903	.913	.913
0.90	.873	.875	.883	.896	.902
0.95	.843	.842	.848	.864	.874
1.00	.800	.796	.799	.818	.833

R_2^2

β / C_{sf}	0.5	1.0	2.0	4.0	8.0
0.80	.284	.719	.837	.770	.684
0.85	.262	.707	.850	.791	.696
0.90	.235	.699	.858	.808	.713
0.95	.205	.684	.858	.820	.729
1.00	.151	.657	.850	.820	.732

R_3^2

β / C_{sf}	0.5	1.0	2.0	4.0	8.0
0.80	.518	.519	.525	.440	.254
0.85	.525	.533	.541	.473	.310
0.90	.516	.538	.555	.503	.355
0.95	.505	.584	.538	.522	.397
1.00	.498	.574	.553	.534	.430

R_w^2

β / C_{sf}	0.5	1.0	2.0	4.0	8.0
0.80	.884	.917	.932	.931	.921
0.85	.884	.917	.932	.933	.926
0.90	.874	.906	.921	.925	.921
0.95	.855	.887	.901	.908	.907
1.00	.820	.859	.873	.882	.884

5.14 The response of the R^2-criteria to C_{sf} and β at Stadar-forsen. (See chapter 5.4; 5.4.5)

5.4.5 The response of the R^2-criteria to Fc, L_p/Fc and β

The danger of letting the R_w^2-criterion define the parameter optimum is accentuated in fig. 5.13. A test plotting was made at:

$$\left.\begin{aligned} Fc &= 150 \text{ mm} \\ L_p &= 150 \text{ mm} \\ \beta &= 4 \end{aligned}\right\}$$

This is the R_w^2-optimum. The model now underestimates γ-flow. From the response surface it is clear that the R_2^2-criterion was deteriorated by this modification of the parameters. This gives an unacceptable error in the accumulated flow after the four calibration years.

The R_{sum}-criterion (chapter 5.1), however, has its optimum at:

$Fc = 150$ mm,

$L_p = 150$ mm,

$\beta = 2$,

which is very close to the original setting.

5.4.6 The response of the R^2-criteria to C_{sf} and β

The R_{sum}-criterion (chapter 5.1) shows optimum (compare fig. 5.14) at:

$\beta = 2.0$,

$C_{sf} = 0.9$.

No test plotting was made, because the original parameter values are close to this optimum, and further more the test plotting of chapter 5.4.5 showed no improvement of the hydrograph.

5.4.7 The response of the R^2-criteria to T_o and C_o

According to fig. 5.15 C_o seemed to be a bit too small, and a test plotting was made at:

$T_o = 0\ ^oC$,

$C_o = 2.3$ mm/(^oC · day).

It shows a small improvement.

R_1^2

C_o	1.4	1.7	2.0	2.3	2.6	2.9	3.2	3.5
T_o								
-1.0	.881	.884	.831	.750	.659	.	.	.
-0.5	.828	.905	.919	.890	.836	.	.	.
0.0	.684	.821	.893	.925	.926	.889	.837	.772
0.5	.452	.637	.762	.843	.890	.903	.903	.873
1.0	.161	.374	.533	.652	.737	.795	.832	.850

R_2^2

C_o	1.4	1.7	2.0	2.3	2.6	2.9	3.2	3.5
T_o								
-1.0	.724	.645	.590	.533	.480	.	.	.
-0.5	.733	.733	.697	.634	.602	.	.	.
0.0	.657	.721	.754	.752	.717	.700	.665	.600
0.5	.597	.639	.707	.761	.755	.741	.725	.725
1.0	.502	.558	.605	.656	.695	.720	.729	.724

R_3^2

C_o	1.4	1.7	2.0	2.3	2.6	2.9	3.2	3.5
T_o								
-1.0	.624	.590	.486	.403	.357	.	.	.
-0.5	.652	.660	.632	.553	.491	.	.	.
0.0	.624	.648	.653	.640	.617	.560	.518	.452
0.5	.569	.520	.585	.616	.616	.605	.593	.562
1.0	.082	.273	.387	.457	.508	.534	.538	.537

R_w^2

C_o	1.4	1.7	2.0	2.3	2.6	2.9	3.2	3.5
T_o								
-1.0	.905	.901	.859	.794	.716	.	.	.
-0.5	.875	.922	.926	.902	.857	.	.	.
0.0	.779	.870	.911	.934	.937	.902	.863	.813
0.5	.633	.757	.838	.887	.918	.935	.916	.895
1.0	.450	.594	.699	.773	.826	.859	.880	.888

Fig. 5.15 The response of the R^2-criteria to T_o (°C) and C_o (mm/(°C · day)) at Stadarforsen. (See ch. 5.4.7)

R_1^2

C_{wh} \ C_{rfr}	0.00	0.05	0.10	0.20	0.40	0.80
0.00	.905	.905	.905	.905	.905	.
0.05	.918	.924	.922	.916	.907	.898
0.10	.924	.918	.912	.901	.876	.845
0.15	.922	.901	.890	.867	.834	.
0.20	.912	.874	.857	.826	.778	.

R_2^2

C_{wh} \ C_{rfr}	0.00	0.05	0.10	0.20	0.40	0.80
0.00	.740	.740	.740	.740	.740	.
0.05	.756	.772	.773	.766	.756	.755
0.10	.773	.784	.782	.773	.746	.726
0.15	.780	.780	.775	.762	.733	.
0.20	.777	.767	.761	.746	.710	.

R_3^2

C_{wh} \ C_{rfr}	0.00	0.05	0.10	0.20	0.40	0.80
0.00	.663	.663	.663	.663	.663	.
0.05	.656	.652	.650	.656	.657	.659
0.10	.649	.648	.651	.651	.638	.625
0.15	.644	.636	.635	.624	.581	.
0.20	.643	.622	.612	.585	.532	.

R_w^2

C_{wh} \ C_{rfr}	0.00	0.05	0.10	0.20	0.40	0.80
0.00	.919	.919	.919	.919	.919	.
0.05	.929	.934	.934	.929	.923	.919
0.10	.935	.933	.930	.923	.907	.888
0.15	.935	.923	.917	.903	.882	.
0.20	.929	.907	.898	.879	.851	.

Fig. 5.16 The response of the R^2-criteria to C_{wh} and C_{rfr} at Stadarforsen. (See chapter 5.4; 5.4.8).

5.4.8 The response of the R^2-criteria to C_{wh} and C_{rfr}

The settings of C_{rfr} and C_{wh} to 0 were assumed to be physically impossible and of only theoretical interest. An optimum setting then seemed to be (fig. 5.16):

$$C_{rfr} = 0.05,$$
$$C_{wh} = 0.05.$$

A plotting was made at this point. The test plotting managed to center the spring floods better than the original plotting and was therefore considered to be better than the original one.

5.5 Results of the study

It is obvious that the R_w^2-criterion is not a good criterion of fit for our purposes. The snowmelt period governs the behaviour of the R_w^2-criterion too much. For example, the β-parameter of Stadarforsen (and to some extent the one of Kultsjön too) is badly optimized by the R_w^2-criterion.

Another disadvantage of the studied criteria is the R_3^2-criterion. It is disturbed by the fact that different parameter settings give different classifications of data. Both the initial variance and the sum of the squared residuals may be greatly changed by this phenomenon. This could lead to a change in R_3^2, not from a change of fit, but from a rearrangement of the data available.

In order to develop an acceptable criterion of fit the sum of the R_1^2, the R_2^2 and the R_3^2-criteria was also studied. The weakness of R_3^2 described above, however, does influence this criterion too.

To overcome this drawback it is suggested that the classification of data should not be changed during comparison of different parameter settings.

STADARFORSEN

Parameter	Original setting	R_1^2-optimum	R_2^2-optimum	R_3^2-optimum	R_{sum}-optimum	R_w^2-optimum
K_2 (1/(s · mm))	350	300	500	350	350	350
C_{perc} (mm/day)	1.0	1.0	1.5	1.0	1.0	1.0
K_1 (1/(s · mm))	3500	1500	3500	3500	3500	3500
C_{route} (days/m^3)	0.0000	0.0000	0.0005	0.0010	0.0000	0.0000
B_{max} (days)	6	5	7	5	5	5
K_o (1/(s · mm))	12500	25000	25000	7500	22500	22500
L_{uz} (mm)	15	30	25	5	25	25
K_o (1/(s · mm))	12500	16500	8500	8500	14500	16500
K_1 (1/(s · mm))	3500	3500	2500	4500	4500	3500
Fc (mm)	150	150	150	150	150	150
L_p/Fc	1.0	1.0	1.0	1.0	1.0	1.0
β	1.5	8.0	2.0	1.0	2.0	4.0
β	1.5	8.0	2.0	1.0	2.0	4.0
C_{sf}	0.90	0.85	0.95	0.85	0.90	0.85
T_o (°C)	0.0	0.0	0.5	- 0.5	0.0	0.0
C_o (mm/(°C · day))	2.0	2.3	2.6	1.7	2.3	2.3
C_{wh}	0.05	0.05	0.10	0.05	0.10	0.05
C_{rfr}	1.0	0.05	0.05	1.0	0.05	0.05

Table 5.2 The optimum parameter settings of Stadarforsen as judged by the different criteria of fit. For comparison the original parameter setting (the optimum of an 8 year period as judged by the calibraters) is also printed in this table.

KULTSJÖN

Parameter	Original setting	R_1^2 optimum	R_2^2 optimum	R_3^2 optimum	R_{sum} optimum	R_w^2 optimum
K_2 (1/(s · mm))	300	600	200	600	450	450
C_{perc} (mm/day)	1.3	3.6	2.[illegible]	2.7	2.4	2.6
K_1 (1/(s · mm))	4000	3000	3000	6000	3000	3000
C_{route} (day s/m^3)	0.00103	0.0005	0.001	0	0.001	0.0005
B_{max} (days)	2	2	2	3	2	2
Fc (mm)	150	200	200	100	200	200
I_p/Fc	1.0	0.6	0.6	0.6	0.6	0.6
β	3.0	1.0	4.0	2.0	4.0	2.0
β	3.0	1.0	4.0	2.0	4.0	2.0
C_{sf}	1.23	1.2	1.1	1.0	1.1	1.1
T_o (°C)	0.5	- 0.5	0.5	0.0	0.0	0.0
C_o (mm/(°C · day))	3.2	2.0	3.5	3.8	2.9	2.6
C_{wh}	0.05	0.05	0.05	0.05	0.05	0.05
C_{rfr}	1.0	1.0	0.05	0.05	0.4	1.0

Table 5.3 The optimum parameter settings of Kultsjön as judged by the different criteria of fit. For comparison the original parameter setting (the optimum of an 8 year period as judged by the calibrators) is also printed in this table.

The optimum parameter settings, as described by the different R^2-criteria and the R_{sum}-criterion, may be studied in tab. 5.2 and 5.3, where they are compared with results from calibrations by visual inspection. Note that the HBV-model is usually calibrated during 8-year periods, but due to the computer capacity only 4-year periods were used in the study of the response surfaces of the R^2-criteria. We see that the R_{sum}-criterion is mostly closer to the original setting than the R^2_w-criterion (tab. 5.4).

In Kultsjön, however, any studied parameter optimum suggested by any of the criteria did not give better hydrographs than the originally plotted one. Possible explanations to this are the bad quality of both the runoff data and the climate data and the incompleteness of the model type used (the lack of a K_o-parameter).

In Stadarforsen the R_{sum}-criterion agrees with the visual inspection surprisingly well. If some sort of fixed classification manages to make the R^2_3-criterion more reliable, it is obvious that the HBV-model could be automatically calibrated in Stadarforsen.

Whether the model can be automatically calibrated for any catchment, is a much harder question. This study covers only two catchments and furthermore only four years of each one.

The impression of the author is that the R_{sum}-criterion or some other linear combination of the R^2-criteria might be the basis of a useful criterion of fit. Other quantities, such as the sum of the residuals and the ratio of over- or underestimations of the hydrograph, may perhaps take part in a criterion of fit too, since these two quantities are often used during the subjective calibration.

	[illegible]		[illegible]	
	R_{sum}	R_w^2	R_{sum}	R_w^2
[illegible]	x	x	x	x
C_{perc}	x	x	x	
K_1	x	x	x	x
C_{route}	x	x	x	
[illegible]$_{max}$	x	x	x	x
K_o	x	x	–	–
L_{uz}	x	x	–	–
K_o	x		[illegible]	–
K_1		x	–	–
Fc	x	x	x	x
L_p/Fc	x	x	x	x
[illegible]	x		x	
[illegible]	x		x	
C_{sf}	x		x	x
T_o	x	x	x	x
C_o	x	x	x	
C_{wh}		x	x	x
C_{rfr}	x	x		x

Table 5.4 A comparison between the R_{sum} and R_w^2 criteria of fit. The criterion which has its optimum closest to the original parameter setting is marked with a cross.

6. CONCLUSIONS

The residuals of the HBV-model are neither independent nor stationary distributed during the year. Yet this has been assumed by many calibrators of hydrological models. A way to get closer to these assumptions is to base a classification of the calibration data on the different processes governing the discharge and to consider each class to be a separate set of residuals. By doing this we do not get rid of the autocorrelation, but the residuals become more stationary distributed. In fact it is impossible to get rid of the autocorrelation of the model residuals, since one single climate measurement error affects the level of the model storage and thereby the discharge during a series of days.

Knowing that a classification helps in making the residuals more stationary, the R_i^2-criterion of fit (chapter 5.1) was computed for each class. The sum of these R_i^2-criteria (the R_{sum}-criterion) showed out to be a better criterion of fit than the formerly used R_w^2-criterion. Concerning the possibility of automatic calibration of the HBV-model at any catchment, data of good quality must be demanded. There must also be a sufficient number of degrees of freedom in the model. It might otherwise compensate an unability to follow the observed hydrograph by producing a too damped hydrograph, overestimating low flows and underestimating high ones.

If these demands are fullfilled, the R_{sum}-criterion gives a better representation of the goodness of fit than the R_w^2-criterion. The response surfaces had mostly a regular elliptic shape. Therefore it seems plausible that an optimization algorithm such as Rosebrock's (1960) method or Powell's (1964) method with slight modifications may perform acceptably.

The demand above of many degrees of freedom contains a dilemma. If a model is equipped with a sufficient number of degrees of freedom, it will be able to reconstruct almost any discharge record from any climate record. But the headpoint in making a model is not to make

it complex in order to fit the calibration period only, (since this is no guarantee for fit during other periods), but to make it simple and yet fit both the calibration period and the independent periods.

APPENDIX A

The distributions of the residuals (differences between the computed and the recorded hydrographs) are shown below. Histograms showing the residuals both separated and not separated by the MSC (chapter 4.1) are plotted.

A description of the method used when constructing these histograms can be found in chapter 4.2. The prescribed minimum period duration is explained in chapter 4.4.

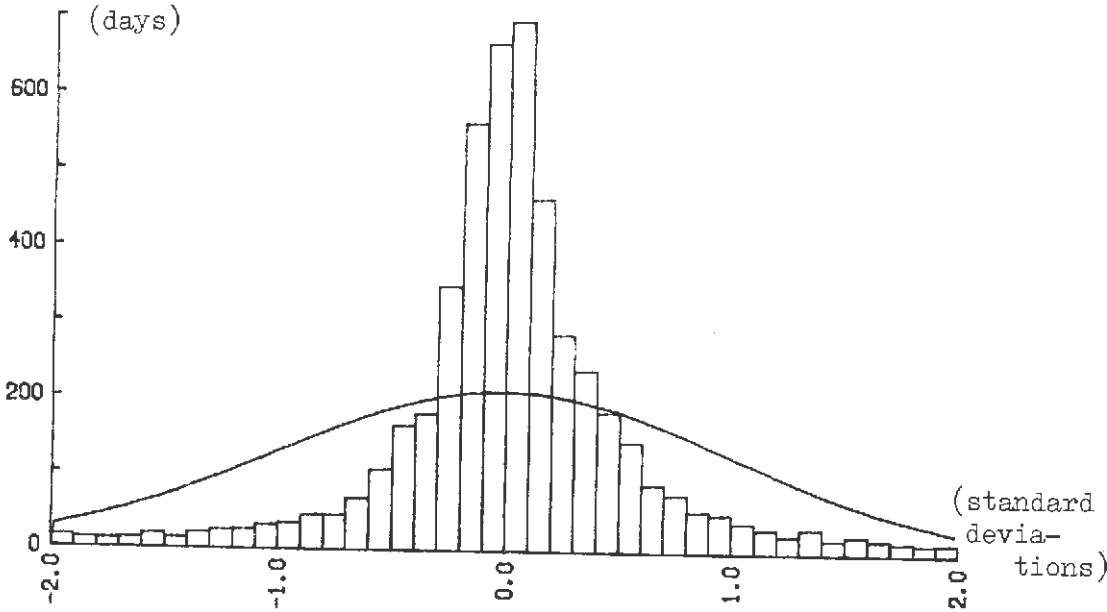

Fig. A.1 Histogram showing the residuals of Stadarforsen 61.10.01 - 76.03.31.
Prescribed minimum period duration: 1 day.
Mean = -589 l/s.
Standard deviation = 22 503 l/s.
Number of residuals = 5 273.
Number of exceeding residuals (NER) = 337.

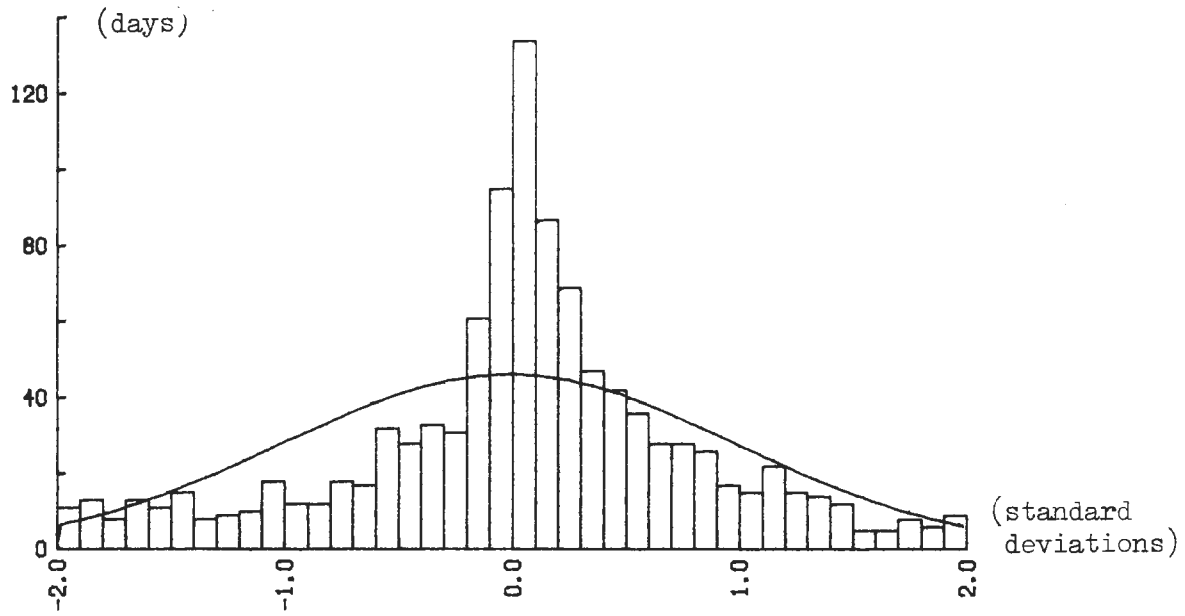

Fig. A.2 Histogram showing the snowmelt residuals of Stadarforsen, 61.10.01 - 76.03.31.
Prescribed minimum period duration: 1 day.
Mean = 1 385 l/s.
Standard deviation = 41 431 l/s.
Number of residuals = 1 156.
NER = 76.

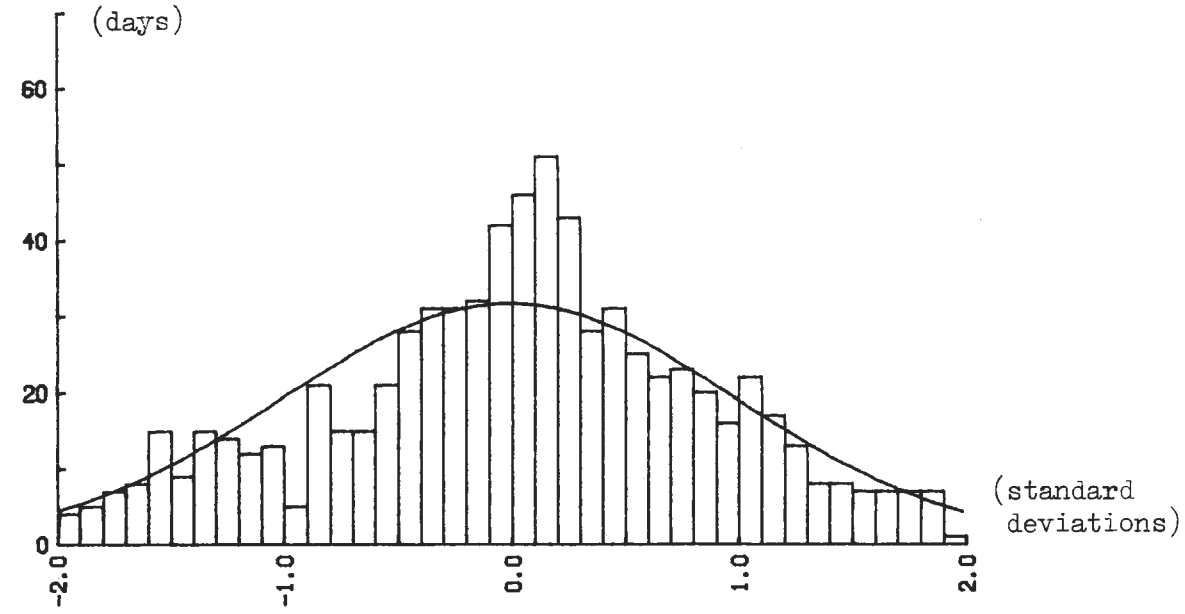

Fig. A.3 Histogram showing the snowmelt residuals of Stadarforsen, 61.10.01 - 76.03.31.
Prescribed minimum period duration: 5 days.
Mean = -4 645 l/s.
Standard deviation = 48 485 l/s.
Number of residuals = 794.
NER = 49.

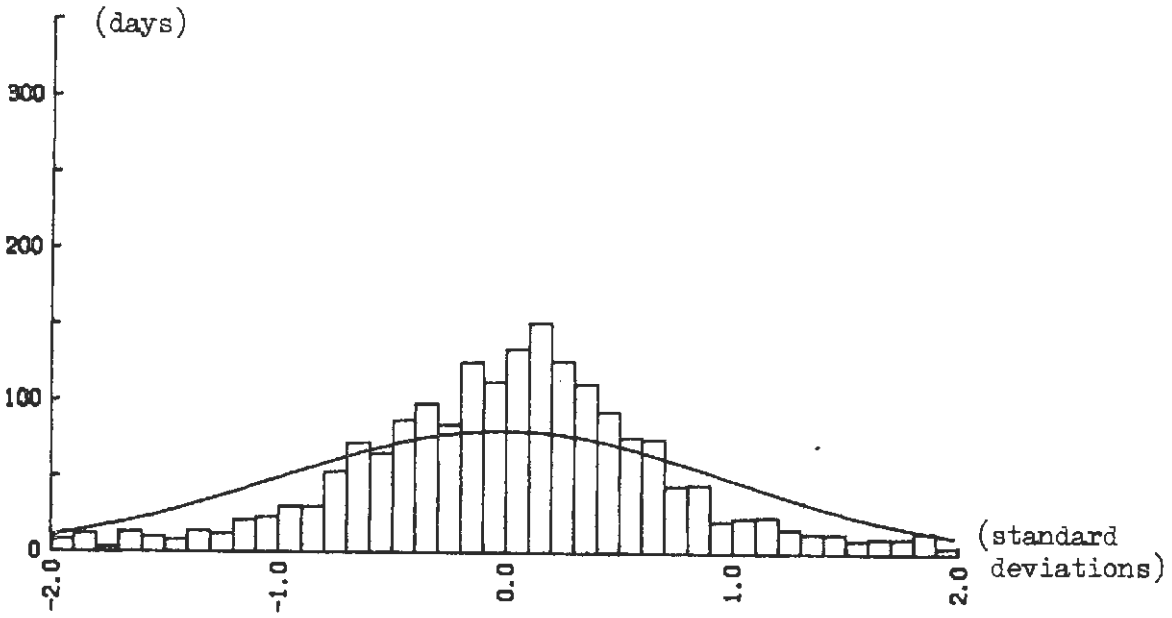

Fig. A.4 Histogram showing the γ-flow residuals of Stadarforsen 61.10.01 - 76.03.31.
Prescribed minimum period duration: 1 day
Mean = 16 l/s.
Standard deviation = 17 553 l/s.
Number of residuals = 2 008.
NER = 116.

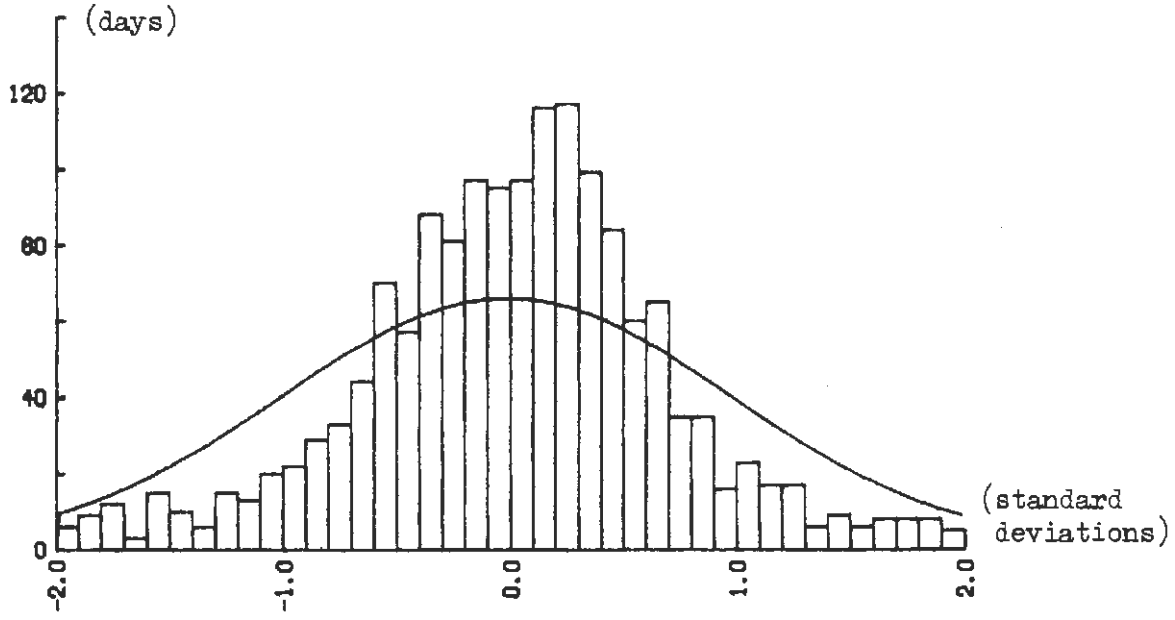

Fig. A.5 Histogram showing the γ-flow residuals of Stadarforsen 61.10.01 - 76.03.31.
Prescribed minimum period duration: 5 days.
Mean = -590 l/s.
Standard deviation = 18 185 l/s.
Number of residuals = 1 650.
NER = 94.

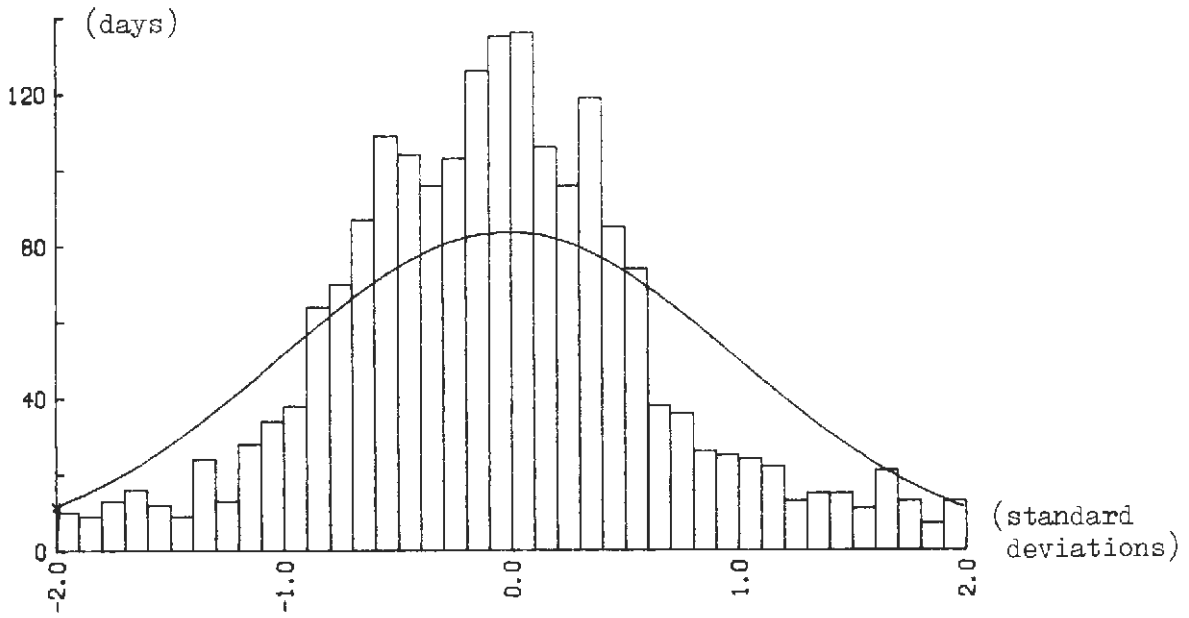

Fig. A.6 Histogram showing the low flow residuals of Stadarforsen 61.10.01 - 76.03.31.
Prescribed minimum period duration: 1 day.
Mean = -743 l/s.
Standard deviation = 5 629 l/s.
Number of residuals = 2 097.
NER = 102.

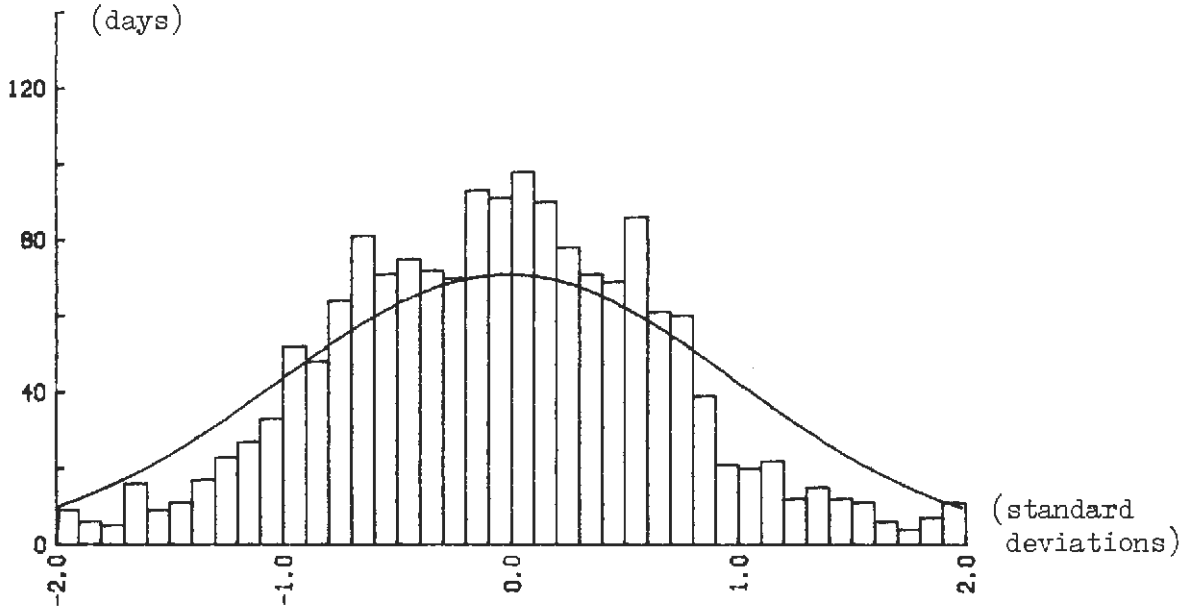

Fig. A.7 Histogram showing the low flow residuals of Stadarm forsen 61.10.01 - 76.03.31.
Prescribed minimum period duration: 5 days.
Mean = 1 188 l/s.
Standard deviation = 4 393 l/s.
Number of residuals = 1 780.
NER = 114.

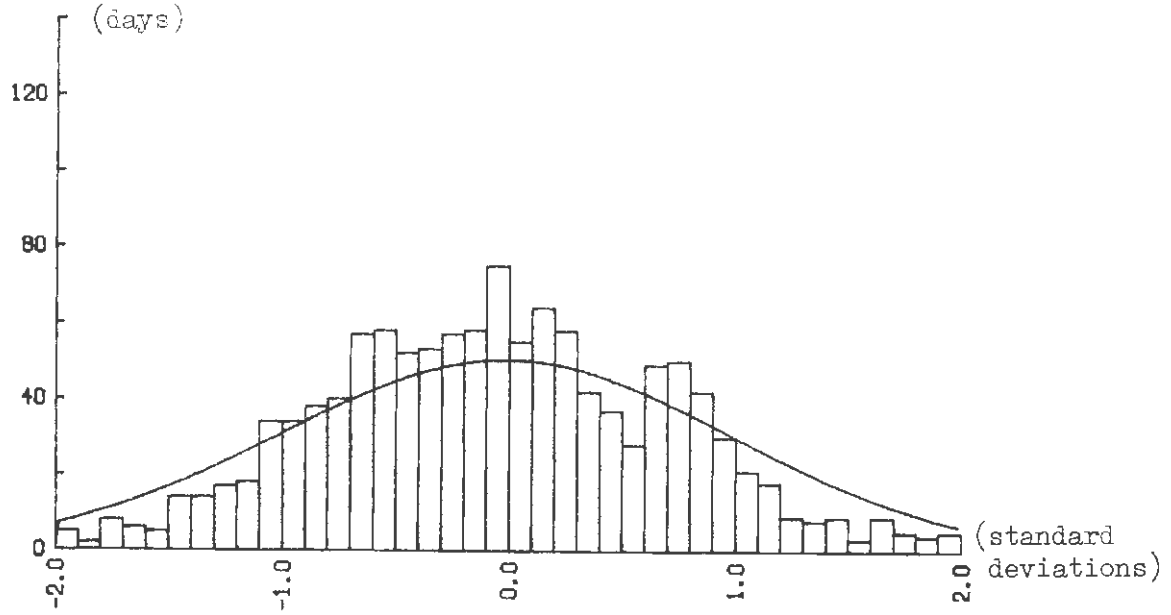

Fig. A.8 Histogram showing the low flow residuals of Stadarforsen 61.10.01 - 76.03.31.
Prescribed minimum period duration: 20 days
Mean = -1 578 l/s.
Standard deviation = 3 890 l/s.
Number of residuals = 1 260.
NER = 69.

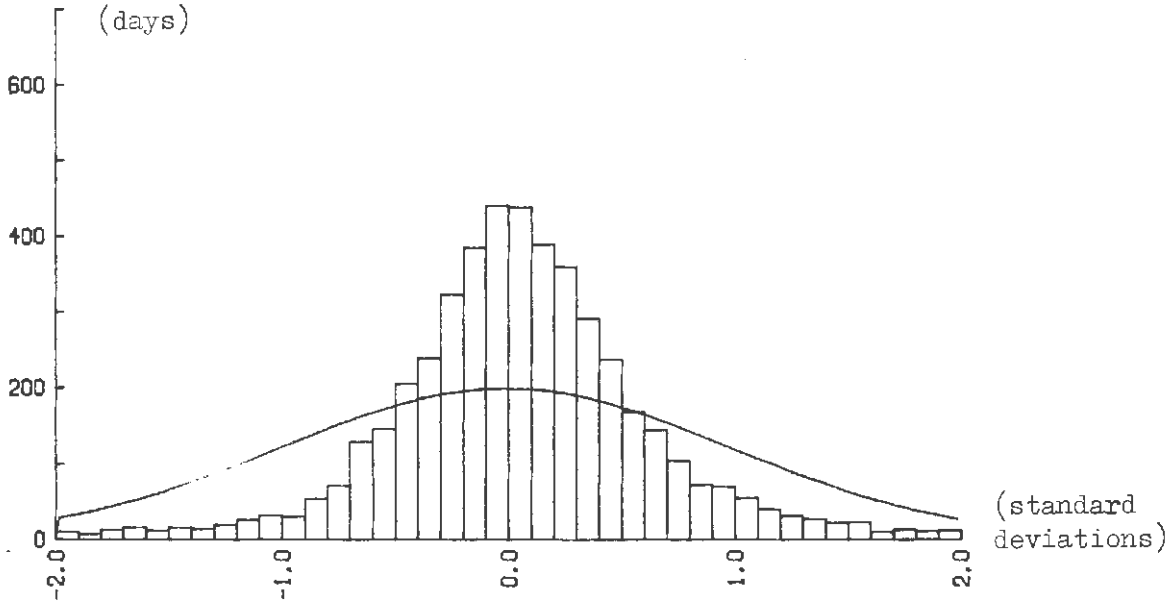

Fig. A.9 Histogram showing the residuals of Kultsjön 62.10.01 - 76.05.18.
Prescribed minimum period duration: 1 day.
Mean = 374 l/s.
Standard deviation = 16 905 l/s.
Number of residuals = 4 977.
NER = 274.

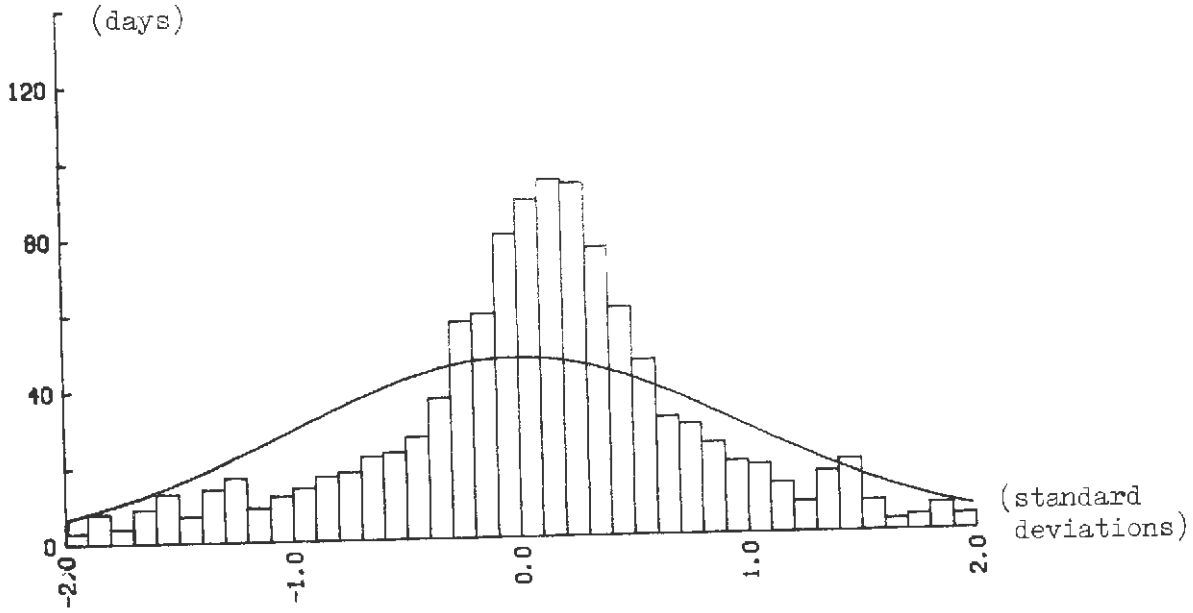

Fig. A.10 Histogram showing the snowmelt residuals of Kultsjön 62.10.01 - 76.05.18.
Prescribed minimum period duration: 1 day
Mean = -545 l/s.
Standard deviation = 30 198 l/s.
Number of residuals = 1 185.
NER = 74.

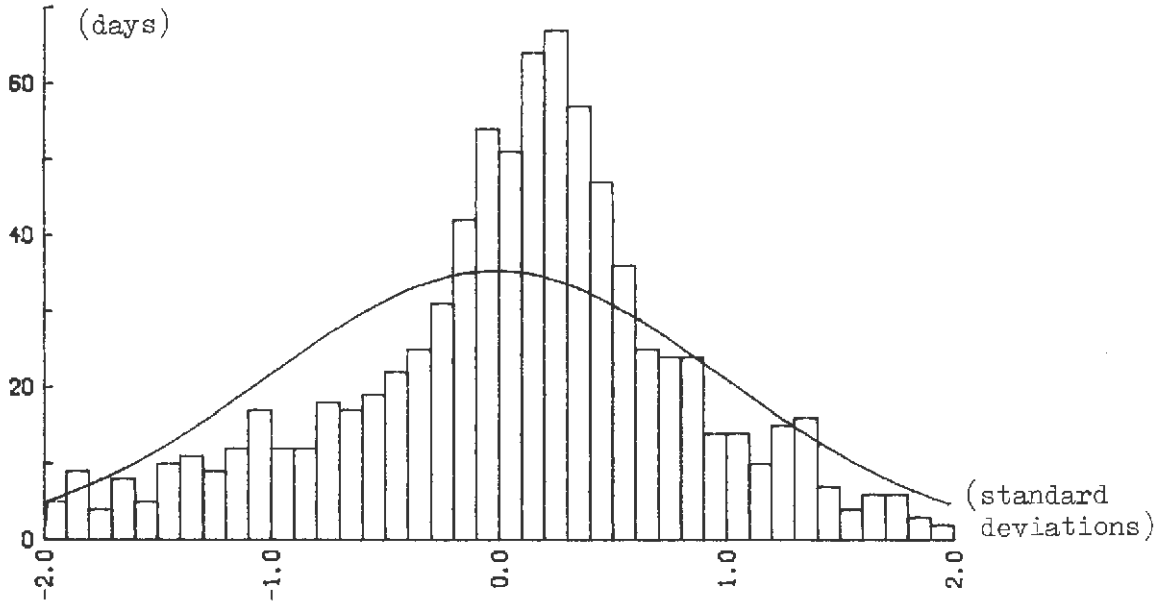

Fig. A.11 Histogram showing the snowmelt residuals of Kultsjön 62.10.01 - 76.05.18.
Prescribed minimum period duration: 5 days.
Mean = -2 400 l/s.
Standard deviation = 33 605 l/s.
Number of residuals = 884.
NER = 50.

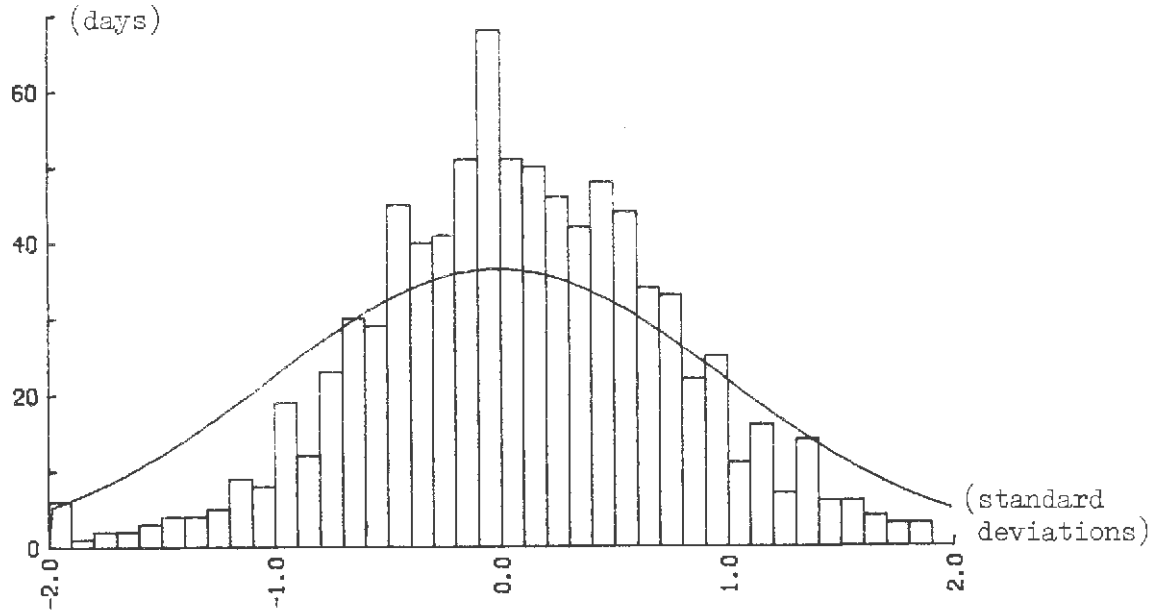

Fig. A.12 Histogram showing the γ-flow residuals of Kultsjön 62.10.01 - 76.05.18.
Prescribed minimum period duration: 1 day.
Mean = 411 l/s.
Standard deviation = 14 652 l/s.
Number of residuals = 914.
NER = 47.

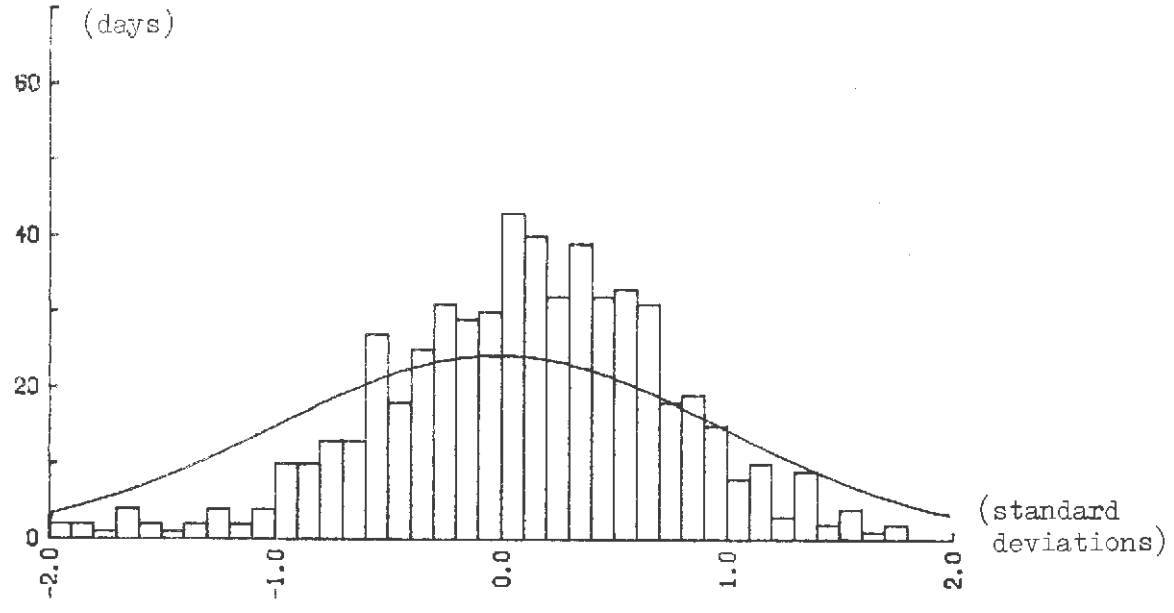

Fig. A.13 Histogram showing the γ-flow residuals of Kultsjön 62.10.01 - 76.05.18.
Prescribed minimum period duration: 5 days.
Mean = 1 178 l/s.
Standard deviation = 16 067 l/s.
Number of residuals = 607.
NER = 36.

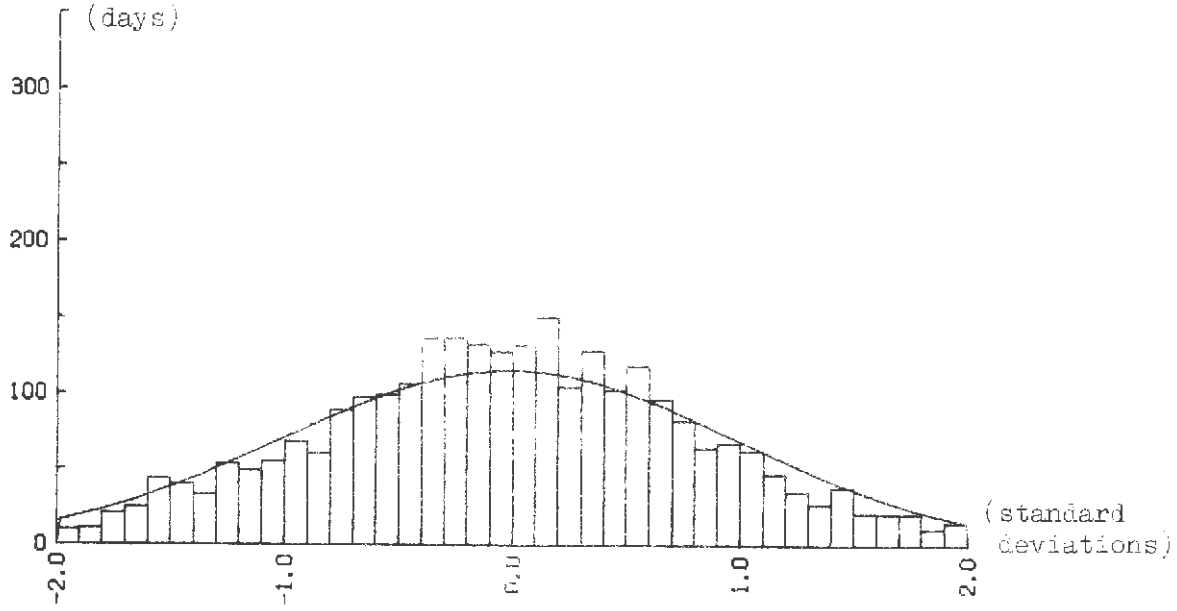

Fig. A.14 Histogram showing the low flow residuals of Kultsjön 62.10.01 - 76.05.18.
Prescribed minimum period duration: 1 day.
Mean = 725 l/s.
Standard deviation = 7 068 l/s.
Number of residuals = 2 876.
NER = 145.

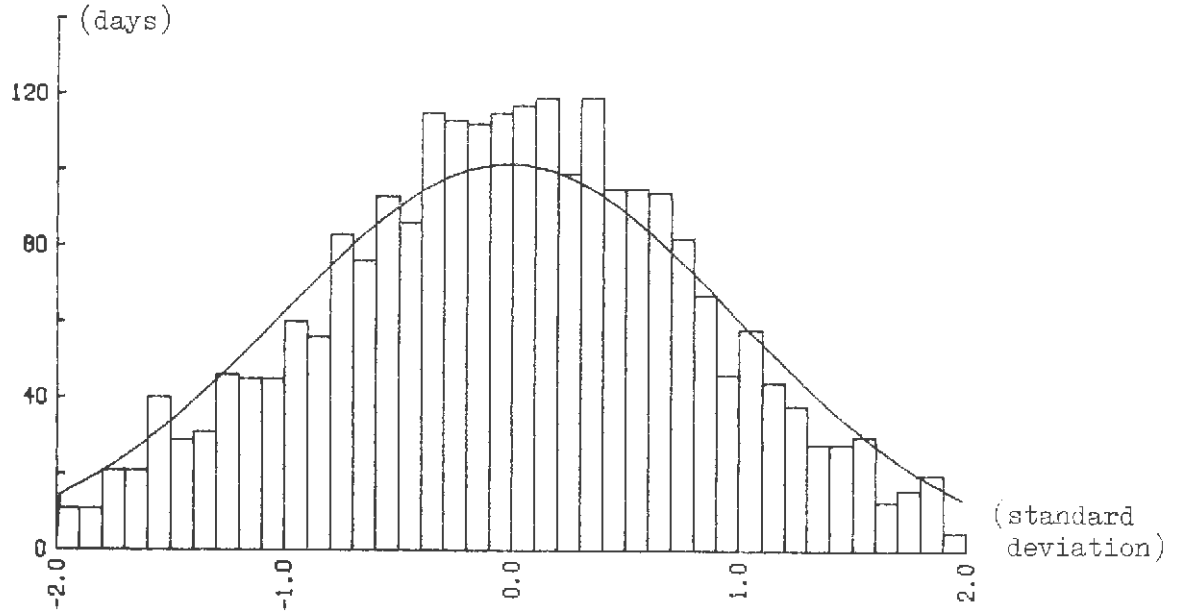

Fig. A.15 Histogram showing the low flow residuals of Kultsjön 62.10.01 - 76.05.18.
Prescribed minimum period duration: 5 days.
Mean = 530 l/s.
Standard deviation = 6 863 l/s.
Number of residuals = 2 545.
NER = 123.

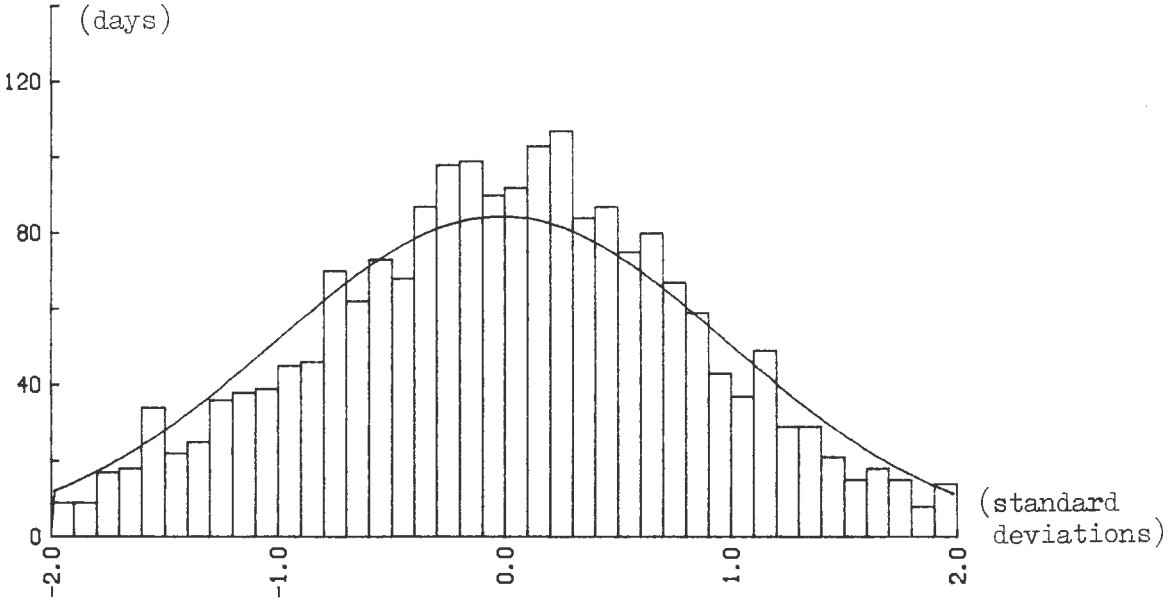

Fig. A.16 Histogram showing the low flow residuals of Kultsjön 62.10.01 - 76.05.18.
Prescribed minimum period duration: 20 days.
Mean = 370 l/s.
Standard deviation = 6 637 l/s.
Number of residuals = 2 117.
NER = 100.

Appendix B

LIST OF SYMBOLS

B_{max}	maximum base in the transformation function
B_q	actual base in the transformation function
C_o	degree-day melt factor
C_{perc}	percolation capacity
C_{rfr}	refreezing coefficient
C_{route}	parameter in the transformation function
C_{sf}	snowfall correction factor
C_{wh}	water holding capacity of snow
E_a	actual evaporation
E_p	potential evaporation
Fc	maximum soil moisture capacity in the model
F_o^2	initial variance
K_o	storage discharge parameter of the upper zone
K_1	slow drainage storage discharge parameter of the upper zone
K_2	storage discharge parameter of the lower zone
L_p	limit for potential evaporation
L_{uz}	limit for slow drainage of the upper zone
M	snowmelt
MSC	mechanism separation criterion
n	total number of observations in a class
N	number of observations in a continous period in a class
NER	number of residuals not contained in the histogram of the estimated density function
N_τ	total number of observations of $R(\tau)$
N_j	duration of period j
n_x	sum of autocorrelation coefficients

P	precipitation
P_{corr}	rainfall correction factor
P_{lapse}	area elevation correction of precipitation
p_i	probability
P_w	part of the lower zone representing wet areas
Q_o	runoff generated from the upper zone
Q_1	slow drainage runoff generated from the upper zone
Q_2	runoff generated from the lower zone
Q_c	computed runoff
Q_g	total generated runoff
Q_r	recorded runoff
$\bar{Q}_r$	mean of recorded runoff
R^2	criterion of fit
R_{sum}	criterion of fit $(R_1^2 + R_2^2 + R_3^2)$
R_w^2	" " " (the material as a whole)
R_1^2	" " " (snowmelt)
R_2^2	" " " (γ-flow)
R_3^2	" " " (low flow)
$R(\tau)$	autocovariance with time step τ
$\hat{R}(\tau)$	estimation of the autocovariance
$\hat{R}_j(\tau)$	estimated autocovariance of residuals separated by τ days for the j:th continuous period
S	standard deviation
S_b	bottom storage under the snowpack
S_{lz}	storage in the lower zone of the model
S_s	storage of snow in the catchment
S_{sm}	soil moisture storage in the model
S_{uz}	storage in the upper zone of the model
T	temperature
T_o	general temperature correction

T_{lapse}	area elevation correction of temperature
t	time
t_j	starting time for the j:th period
U	test variable
Var(X)	variance of the stochastic variable X
X	a residual regarded as a stochastic variable
$\overline{X}$	mean value of the residuals
β	parameter of the soil moisture zone
γ	indicates rain or recession succeeding rain or snowmelt
μ	mean value
σ	standard deviation
τ	time step

LIST OF REFERENCES

Andersson, R L (1941) — Distribution of serial correlation coefficient. Ann. Math. Statist. 8 No. 1

Bergström, S (1976) — Development and application of a conceptual runoff model for Scandinavian catchments. SMHI Rapporter Hydrologi och Oceanografi Nr RHO 7

Clarke, R T (1973) — A review of some mathematical models used in hydrology, with observation on their calibration and use. Journal of Hydrology No. 19

Hamon & Hannan (1963) — Estimating relations between time series. J. Geophys. Res., 81 (21). 6033-6041

Hansen, E (1971) — Analyse af hydrologiske tidsserier. Laboratoriet for Hydraulik, Danmarks Tekniske Højskole

Hjorth, U (1976) — Stokastiska processer. Kompendium i matematisk statistik III. Matematiska institutionen, Universitetet i Linköping.

Jenkins & Watts (1961) — Spectral analysis and its applications

Kendall & Stuart (1967) — The advanced theory of statistics. Vol. 2, 2nd Edn

Nash & Sutcliffe (1970) — River flow forecasting through conceptual models. Part I. A discussion of principles. Journal of Hydrology No. 10

Powell, M J D (1964) — An efficient method of finding the minimum of a function of several variables without calculating derivates. The Computer Journal, Vol. 7, p. 155

Rosenbrock, H H (1960) — An automatic method for finding the greatest or least value of a function. The Computer Journal, Vol. 3, p. 175

Rudemo & Råde (1970) — Sannolikhetslära och statistik med tekniska tillämpningar. Del 1

Notiser och preliminära rapporter

Serie HYDROLOGI

Nr 1 Sundberg-Falkenmark, M
Om isbärighet.
Stockholm 1963

Nr 2 Forsman, A
Snösmältning och avrinning.
Stockholm 1963

Nr 3 Karström, U
Infrarödteknik i hydrologisk tillämpning:
Värmebilder som hjälpmedel i recipientundersökningar.
Stockholm 1966

Nr 4 Moberg, A
Svenska sjöars isläggnings- och islossningstidpunkter
1911/12 - 1960/61. Del 1. Redovisning av observationsmaterial.
Stockholm 1967.

Nr 5 Ehlin, U & Nyberg, L
Hydrografiska undersökningar i Nordmalingsfjärden.
Stockholm 1968

Nr 6 Milanov, T
Avkylningsproblem i recipienter vid utsläpp av kylvatten.
Stockholm 1969

Nr 7 Ehlin, U & Zachrisson, G
Spridningen i Vänerns nordvästra del av suspenderat materiel
från skredet i Norsälven i april 1969.
Stockholm 1969

Nr 8 Ehlert, K
Mälarens hydrologi och inverkan på denna av alternativa
vattenavledningar från Mälaren.
Stockholm 1970

Nr 9 Ehlin, U & Carlsson, B
Hydrologiska observationer i Vänern 1959 - 1968
jämte sammanfattande synpunkter.
Stockholm 1970

Nr 10 Ehlin, U & Carlsson, B
Hydrologiska observationer i Vänern 17 - 21 mars 1969.
Stockholm 1970

Nr 11 Milanov, T
Termisk spridning av kylvattenutsläpp från Karlshamnsverket.
Stockholm 1971

Nr 12 Persson, M
Hydrologiska undersökningar i Lappträskets representativa
område. Rapport I.
Stockholm 1971.

Nr 13 Persson, M
Hydrologiska undersökningar i Lappträskets representativa
område. Rapport II: Snömätningar med snörör och snökuddar.
Stockholm 1971.

Nr 14 Hedin, L
Hydrologiska undersökningar i Velens representativa område. Beskrivning av området, utförda mätningar samt preliminära resultat. Rapport I.
Stockholm 1971

Nr 15 Forsman, A & Milanov, T
Hydrologiska undersökningar i Velens representativa område. Markvattenstudier i Velenområdet. Rapport II.
Stockholm 1971

Nr 16 Hedin, L
Hydrologiska undersökningar i Kassjöåns representativa område. Nederbördens höjdberoende samt kortfattad beskrivning av området. Rapport I.
Stockholm 1971

Nr 17 Bergström, S & Ehlert, K
Stochastic Streamflow Synthesis in the Velen representative Basin.
Stockholm 1971

Nr 18 Bergström, S
Snösmältningen i Lappträskets representativa område som funktion av lufttemperaturen.
Stockholm 1971

Nr 19 Holmström, H
Test of two automatic water quality monitors under field conditions.
Stockholm 1972

Nr 20 Wennerberg, G
Yttemperaturkartering med strålningstermometer från flygplan över Vänern under 1971.
Stockholm 1971

Nr 21 Prych, A
A warm water effluent analyzed as a buoyant surface jet.
Stockholm 1972

Nr 22 Bergström, S
Utveckling och tillämpning av en digital avrinningsmodell.
Stockholm 1972

Nr 23 Melander, O
Beskrivning till jordartskarta över Lappträskets representativa område.
Stockholm 1972

Nr 24 Persson, M
Hydrologiska undersökningar i Lappträskets representativa område. Rapport III: Avdunstning och vattenomsättning.
Stockholm 1972

Nr 25 Häggström, M
Hydrologiska undersökningar i Velens representativa område. Rapport III: Undersökning av torrperioderna under IHD-åren fram t.o.m. 1971.
Stockholm 1972

Nr 26 Bergström, S
The application of a simple rainfall-runoff model to a catchment with incomplete data coverage.
Stockholm 1972

Nr 27 Wändahl, T & Bergstrand, E
Oceanografiska förhållanden i svenska kustvatten.
Stockholm 1973

Nr 28 Ehlin, U
Kylvattenutsläpp i sjöar och hav.
Stockholm 1973

Nr 29 Andersson, U-M & Waldenström, A
Mark- och grundvattenstudier i Kassjöåns representativa område.
Stockholm 1973

Nr 30 Milanov, T
Hydrologiska undersökningar i Kassjöåns representativa område.
Markvattenstudier i Kassjöåns område. Rapport II.
Stockholm 1973

SMHI Rapporter

HYDROLOGI OCH OCEANOGRAFI

Nr RHO 1
Weil, J G
Verification of heated water jet numerical model.
Stockholm 1974

Nr RHO 2
Svensson, J
Calculation of poison concentrations from a hypothetical accident off the Swedish coast.
Stockholm 1974

Nr RHO 3
Vasseur, B
Temperaturförhållanden i svenska kustvatten.
Stockholm 1975

Nr RHO 4
Svensson, J
Beräkning av effektiv vattentransport genom Sunninge sund till Byfjorden.
Stockholm 1975

Nr RHO 5
Bergström, S & Jönsson, S
The application of the HBV-model to the Filefjell research basin.
Norrköping 1976

Nr RHO 6
Wilmot, W
A numerical model of the effects of reactor cooling water on fjordcirculation, I och II (bilaga till I).
Norrköping 1976

Nr RHO 7
Bergström, S
Development and application of a conceptual runoff model for Scandinavian catchments.
Norrköping 1976

Nr RHO 8
Svensson, J
Seminars at SMHI 1976-03-29--04-01 on Numerical Models of the Spreading of Cooling Water
Norrköping 1976

Nr RHO 9
Simons, J & Funkquist, L & Svensson, J
Application of a numerical model to Lake Vänern
Norrköping 1977

Nr RHO 10
Svensson, S
A Statistical Study for Automatic Calibration of a Conceptual Runoff Model
Norrköping 1977